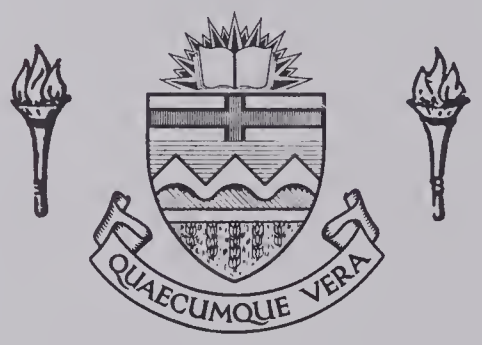

THE UNIVERSITY OF ALBERTA

A PROPOSAL FOR THE EQUALIZATION OF THE MICROELECTRODE IN THE MEASUREMENT OF BIO-ELECTRIC ACTION POTENTIALS USING A DISTRIBUTED PARAMETER R-C NETWORK

by

© Ronald Mitchell Kachman

A THESIS

SUBMITTED TO THE FACULTY OF GRADUATE STUDIES

IN PARTIAL FULFILMENT OF THE REQUIREMENTS FOR THE DEGREE

OF MASTER OF SCIENCE

DEPARTMENT OF ELECTRICAL ENGINEERING

EDMONTON, ALBERTA

FALL, 1970

UNIVERSITY OF ALBERTA

FACULTY OF GRADUATE STUDIES

The undersigned certify that they have read, and recommend to the Faculty of Graduate Studies for acceptance, a thesis entitled "A Proposal for the Equalization of the Microelectrode in the Measurement of Bio-Electric Action Potentials Using a Distributed R-C Network" submitted by Ronald Mitchell Kachman in partial fulfilment of the requirements for the degree of Master of Science.

ABSTRACT

The micropipette capillary electrode is being used extensively in current physiological research in the measurement of the action potentials of nerve and muscle cells. Electrically, the electrode is equivalent to a distributed low-pass R-C transmission line which will distort, in a definite way, any applied potential. In the past, based on a very approximate equivalent circuit, the generation of negative capacity at the amplifier input has been used to approximately compensate for this distortion. However, the best negative capacity adjustment differed from an exact neutralization of the input capacity. This investigation is concerned with a compensation scheme employing the principles of network equalization and a distributed R-C network which will allow a signal entering the microelectrode to reach the output undistorted.

The partial differential equation relating voltage, position and time, which characterizes the general distributed R-C line, has variable coefficients and leads to a situation which is easily solved only in a small number of cases. The specialized equation for the particular line of interest is solved and the steady-state solutions for voltage and current presented. On this basis the z-parameters characterizing the network are derived. A parallel analysis, which by-passes the solution of the equation, is used to derive

the voltage transfer function of the network which yields information regarding the time domain behavior of the line and forms the basis for a stability analysis.

ACKNOWLEDGEMENTS

The research described in this thesis was carried out at the Department of Electrical Engineering, University of Alberta, under the supervision of E. M. Edwards to whom the author is indebted for his guidance and assistance. The author would also like to thank his wife and parents for their encouragement and moral support.

The author is further indebted to the National Research Council and the University of Alberta for financial assistance.

TABLE OF CONTENTS

LIST OF FIGURES

LIST OF TABLES

CHAPTER I

INTRODUCTION

1.1 General

In the field of current physiological research, and within the scope of biomedical electronics, a topic of considerable investigation in the last fifteen years has been the measurement of the bioelectric potentials of nerve and muscle cells.[1-9] The measurement of these potentials has been made possible by the development of the glass capillary microelectrode with a tip diameter of 0.5 microns or less.[3] An electrode of these dimensions allows most of the cells of interest to be penetrated without undue damage and results in highly consistent measurements.

Measurements with small electrodes, however, mean complex electronic problems. Subsequent amplifying stages must meet very difficult and exacting specifications[1,11,12,13] and the distributed R-C, low-pass character of the microelectrode in its measuring environment introduces distortion which must be compensated. With the application of new circuit techniques and field-effect transistors with low noise figures, present-day physiological amplifiers are as sufficient as today's state-of-the-art permits.[11,13]

The aspect of the physiological amplifier which concerns this particular investigation is the correction of

the waveform distortion which is introduced by the micropipette electrode. Several methods are available to the designer and the three most important are discussed in a paper presented by Amatniek.[1] The method which has been accepted by most designers and which has met the specifications with the highest degree of success employs input capacity neutralization. However, certain limitations are still present and some distortion is inherent with this method. With the growing importance of measuring the cellular potentials with increased accuracy, it was considered within reason to search for some improved means of acheiving the desired compensation.

The remainder of this chapter is concerned with a more detailed analysis of the problem and lays the basis for a scheme of compensation which employs the principles of network equalization.

1.2 Physiological Importance of Measurements

All living tissue, in particular the tissues of nerve and muscle cells, are minute generators of electricity. Due to the differing ionic content of the intracellular and extracellular fluids a potential difference (resting potential) exists across the walls of all cells. In the case of excitable tissue, such as nerve and muscle, action potentials can be stimulated and are associated with the depolarization of the cell wall. These transient potentials may have a rate

of rise up to 1000 v/sec[10,12] (rise time of 100 μsec for a 100 mv pulse) and may last as long as 20 msec[5] with 1 msec being typical. The action potential is associated with the passage of an impulse along the nerve fiber or with the contraction of a muscle fiber, and forms the basis of much research in neurophysiology. The measurement of electrical potential gradients across living membranes has aided in a better understanding of the ion transport mechanisms involved. The accurate measurement of resting and action potentials constitutes a valuable aid towards a fuller understanding of the bioelectric nature of living tissue.

1.3 The Capillary Microelectrode

Both resting and action potentials in intracellular measurements are of interest in cellular research today. The capillary microelectrode is used widely because of its ability to record both simultaneously. However, if one is interested in extracellular records and rapid changes of potential, the metal-tip microelectrode can be used to advantage.[7]

Before the time of Ling and Gerard,[3] capillary electrodes of tip diameter 2-5 microns were used in the measurement of cell membrane potentials; the insertion into a fiber caused obvious damage. In 1949, Ling and Gerard developed and perfected methods for drawing and filling microelectrodes of well under one micron tip diameter and were rewarded by

obtaining highly consistent membrane potentials. In 1953 Alexander and Nastuk[6] developed a mechanical electrode puller which produced a more consistent group of electrodes at improved yield. Microelectrodes are seldom drawn by hand today.

Capillary microelectrodes today are characterized by the following properties:

1. Microelectrodes are usually formed from a hard borosilicate glass, usually Pyrex or Phoenix, to ensure strength and minimum chemical reaction with the the cellular fluid.
2. A two-stage mechanical (solenoid) draw is used to achieve constant and repeatable results.
3. The ratio of lumen to wall thickness remains approximately constant to the very tip.
4. Capillary has a fine taper (terminal 2mm) with a gradient of 1/60 to 1/10.
5. Tip outer diameters are 0.5 to 1 micron to ensure minimum cell damage.
6. Microelectrodes are filled with 3 M KCl resulting in comparatively low tip resistance and minimum reaction with the cellular fluid.
7. Electrode resistance may vary from 5 to 50 megohms, but is usually around 20 megohms.
8. Capacitance of the electrode is approximately 1 pf. per mm. of length.

A capillary microelectrode produced from a two-stage mechanical draw is represented diagrammatically in Fig. I-1.

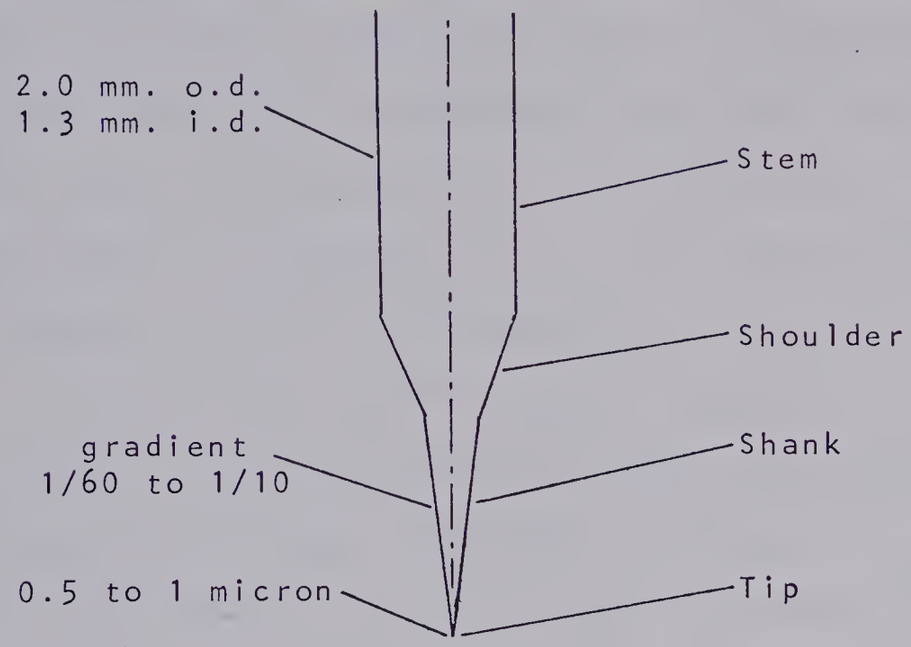

Figure I-1
Pictorial Representation of Microelectrode

1.4 Measuring with Microelectrodes

To study the electrical activity of individual cells the fluid-filled capillary microelectrode is introduced into the interior and the potential difference across the cell wall determined. The tissue is bathed in Ringer's fluid with the bath earthed. A metal electrode, usually Ag-AgCl, is placed in the bath, away from the tissue, where the chemical environment is not subject to variation. To compensate potentials at the metal-fluid junctions another Ag-AgCl electrode is connected to the microelectrode filled with 3 M KCl. The use of 3 M KCl as the capillary electrolyte ensures low tip resistance and a low diffusion potential at the fluid

tip junction. The glass capillary microelectrode serves as an electrolyte bridge between the interior of the cell and the Ag-AgCl electrode; a fluid junction is established at the tip within the cell. Both metal electrodes are connected to the input of the amplifier. An illustration of the measuring setup is provided in Fig. I-2. The electrode is usually mounted as close as possible to the amplifier input in order to improve the high frequency response of the recording system. Various screening schemes are employed to reduce stray capacitances. Excellent references concerning microelectrodes and their use are Cater and Silver,[7] Gesteland, et. al,[8] and Kennard.[9]

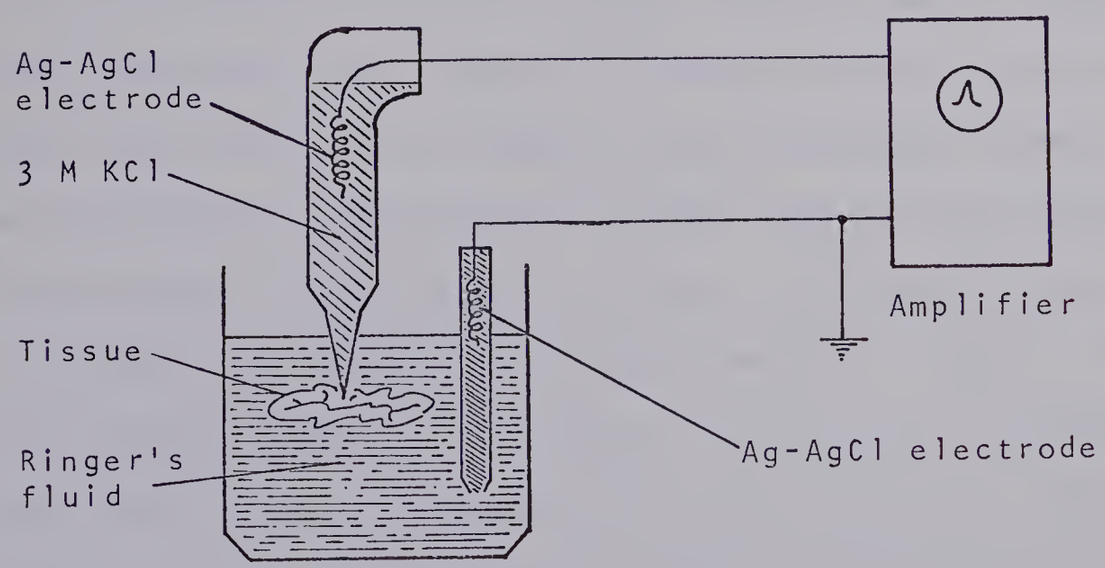

Figure I-2
Arrangement for Measuring with Microelectrodes

1.5 Previously Proposed Equivalent Circuits

To facilitate some scheme of compensation for the distortion that the low-pass character of the capillary microelectrode introduces, the designer must have available some equivalent electrical representation of the electrode in its measuring environment. Two researchers, Woodbury[4] and Amatniek[1] have presented models.

Woodbury's model assumes that the resistance of the electrode and the capacity between the internal and external conducting media make the capillary microelectrode, electrically, a continuous R-C transmission line. The model is presented in Fig. I-3(a) and the numerical values are based on assuming a total electrode resistance of 50 megohms and that the electrode is conical in shape with a slope of 1/66. Capacitance per unit length is constant based on the assumption that the ratio of lumen to wall thickness remains constant throughout. He further assumes that the resistances and capacitances of the circuit in Fig. I-3(a) can be combined to yield the more approximate circuit of Fig. I-3(b). With stray capacitances in the range of 2 → 20 pf, the microelectrode is characterized with a time constant in the range of 0.2 → 1 msec and provides severe distortion to an action potential with a rise time of 100 μsec.

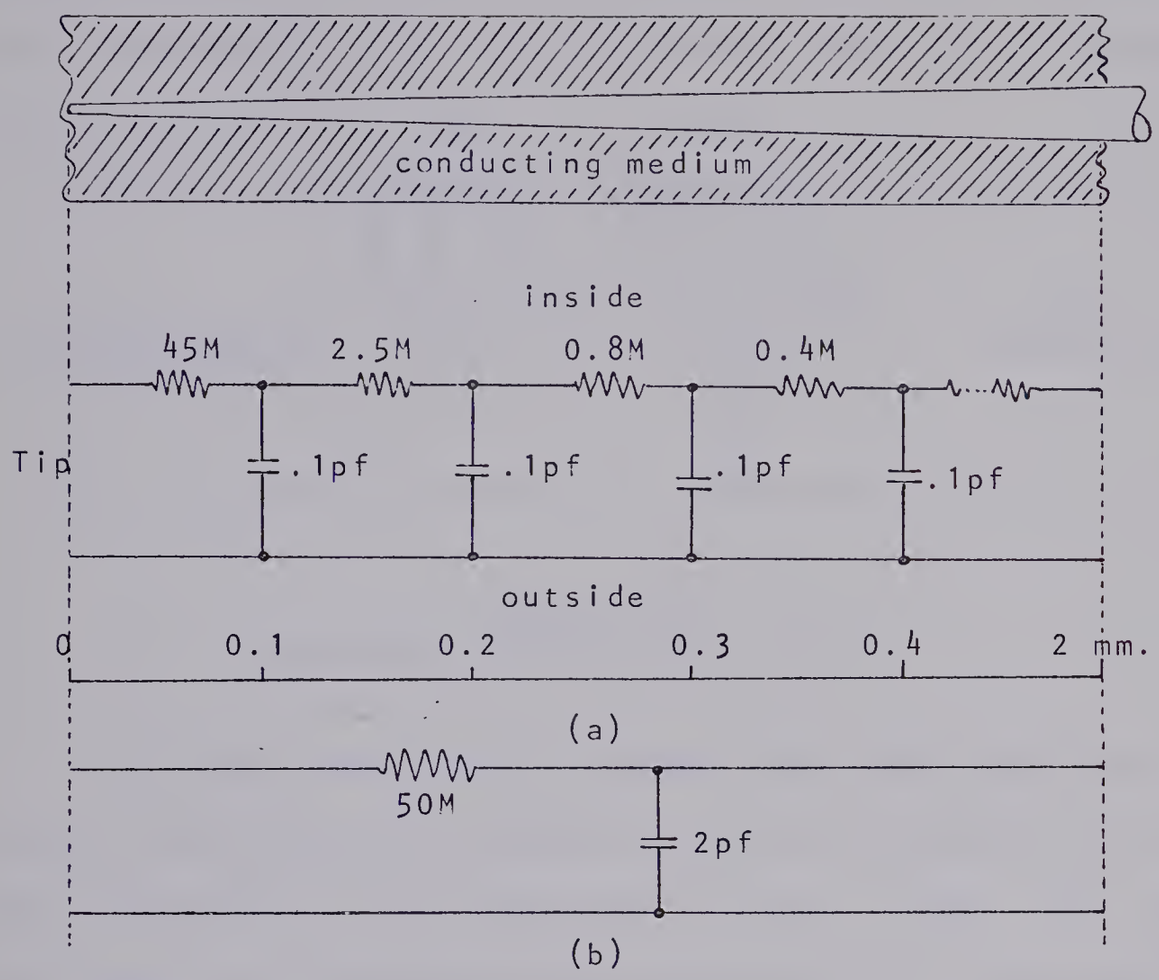

Figure 1-3
Woodbury's Equivalent Circuit

Amatniek presents a more sophisticated model which is derived by dividing the analysis of the microelectrode into three segments: region (c), the portion of the microelectrode within the cell, contains most of the electrode resistance; region (d), the region surrounded by external fluid, contains some of the electrode resistance; and region (e), the portion in air, contains very little electrode resistance. Distributed capacitances are present along the resistances in a

low-pass manner. The capacity and resistance of region (e) may be neglected. Fig. I-4 illustrates Amatniek's proposal.

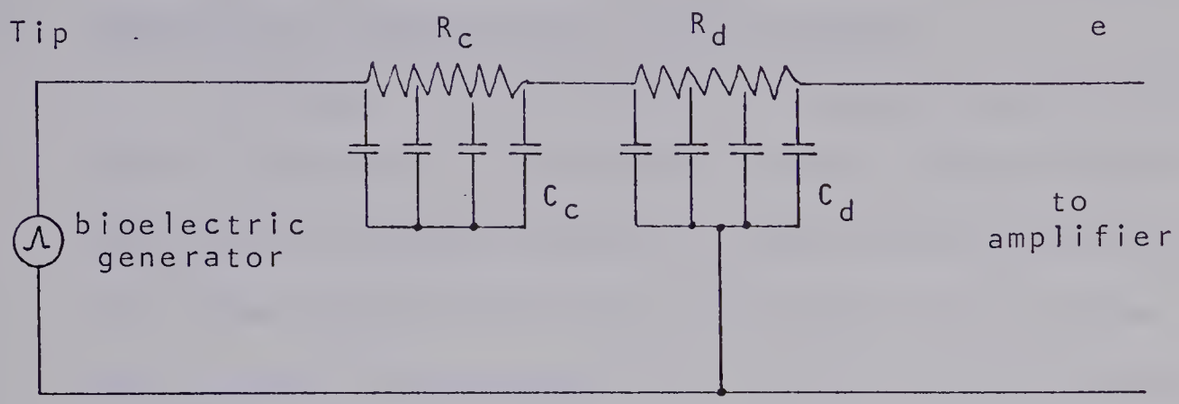

Figure I-4
Amatniek's Equivalent Circuit

Previous compensation schemes have been based on a simple, two-element R-C low-pass network representation similar to Woodbury's as illustrated in Fig. I-3(b). The resistance was the total electrode resistance while the capacitance was a lumped sum of total electrode capacitance, stray capacitance and amplifier input capacitance.

1.6 Methods of Reducing Distortion

The action potential from a nerve or muscle cell may last anywhere from 500 μsec to 20 msec with a rise time as small as 30 μsec. Some method of reducing the distortion introduced by the low-pass microelectrode is necessary if the high frequency changes of potential are to be followed accurately. There are three theoretically feasible methods for restoring the undistorted waveform: decreasing electrode

resistance, decreasing electrode capacitance (including capacity neutralization), and equalizing the overall response.[1]

1.6.1 Reduction of Capacitance and Resistance

If both the resistance and capacitance of the input circuit to the amplifier can be reduced sufficiently, the input circuit will be characterized by a fast time constant (10 μsec required to ensure that the recorded action potential is but a little distorted)[12] and the undistorted waveform can be restored. We are forced to tolerate high resistance microelectrodes (in the order of 20 megohms) since small tip diameters and low shank gradients are necessary for cell penetration with minimal damage. Capacitance reduction has been accomplished using sophisticated electrode fabrication techniques, shielding of input leads and special amplifier design techniques. By far the most successful means of reducing input capacity has been capacity neutralization.

1.6.2 Capacity Neutralization

Capacity neutralization is based on the following simple principle: two capacities of the same magnitude but opposite polarity, when paralleled, will neutralize or cancel each other. The essential element of the neutralized amplifier is the generation of a negative capacity at its input terminals. This is

easily obtained via the Miller effect when output-to-input capacitive feedback is used. The input capacity is easily balanced to a value close to zero by adjusting the feedback capacitor. Continuous compensation, which may be necessitated by in-experiment changes in the equivalent input circuit (due to such factors as tip breakage or tip clogging), is easily monitored. Restoration with capacity neutralization applied has yielded overall time constants in the order of 8 μsec for a 9 megohm electrode.(8)

However, certain limitations are still present and some distortion is inherent with this method. One possible cause of this distortion is that the generated negative capacity, which is assumed to be pure reactance is in fact a complex impedance and closely approximates a negative capacity over only a limited bandwidth. Also, the two-element R-C low-pass equivalent circuit is a very simplified and approximate version of the actual network. Even if the input capacity of the amplifier were in fact neutralized, there still could be waveform distortion due to the remaining distributed constants. In this case the best negative capacity adjustment might be different from an exact neutralization of input capacity.

1.6.3 Equalization

Another method of compensation, discussed by Amatniek[1] and used by Woodbury,[4] is that of network equalization. This method involves the introduction into the amplifier of a transfer characteristic inverse to that of the low-pass capillary microelectrode producing a flat overall response. In Fig.1-5 a block diagram of an equalization circuit is shown where the reciprocal transfer characteristic of the microelectrode is introduced between two stages of the amplifier. Previous usage of this method assumed the two-element equivalent circuit as shown and Woodbury was able to realize overall system time constants in the order of 40 μsec for a 22 megohm electrode.

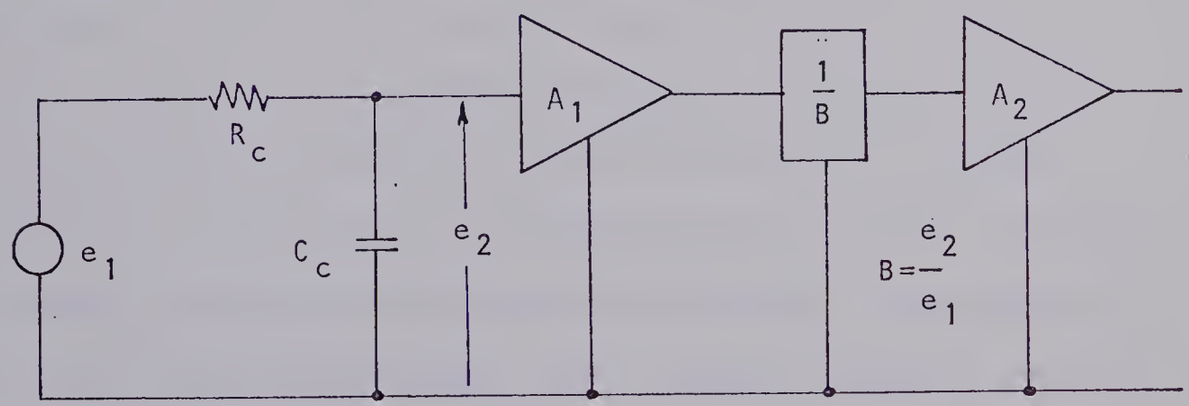

Figure 1-5
Compensation by Equalization

The generation of the reciprocal transfer function can be accomplished by placing a circuit with a

transfer characteristic approximately equal to that of the microelectrode in an input-to-output feedback loop of an operational amplifier. Even with the operational realization of such a circuit the method suffers one major drawback. If the electrode resistance changes due to clogging, tip breakage, or changing electrolyte concentration the low-pass cutoff frequency also changes, and therefore the equalizing network must be readjusted. If the equalization is not continuously monitored and the change takes place in the middle of an experiment, incorrect results may be recorded unknowingly.

1.7 Proposed Scheme of Waveform Restoration

Since the fluid-filled capillary microelectrode behaves electrically like a continuous R-C transmission line (section 1.5), it is considered feasible to achieve waveform restoration by employing the principles of network equalization using thin-film distributed parameter circuits. If feasible, such an evolution would have the advantage of producing, with more accuracy, the inverse transfer characteristics required to equalize the overall response. Also, equalization is superior to capacity neutralization from the viewpoint of noise considerations.[1] The proposed equalization scheme is illustrated in Fig. I-6. Fig. I-6(a) illustrates the entire scheme in block form. V_1 corresponds to

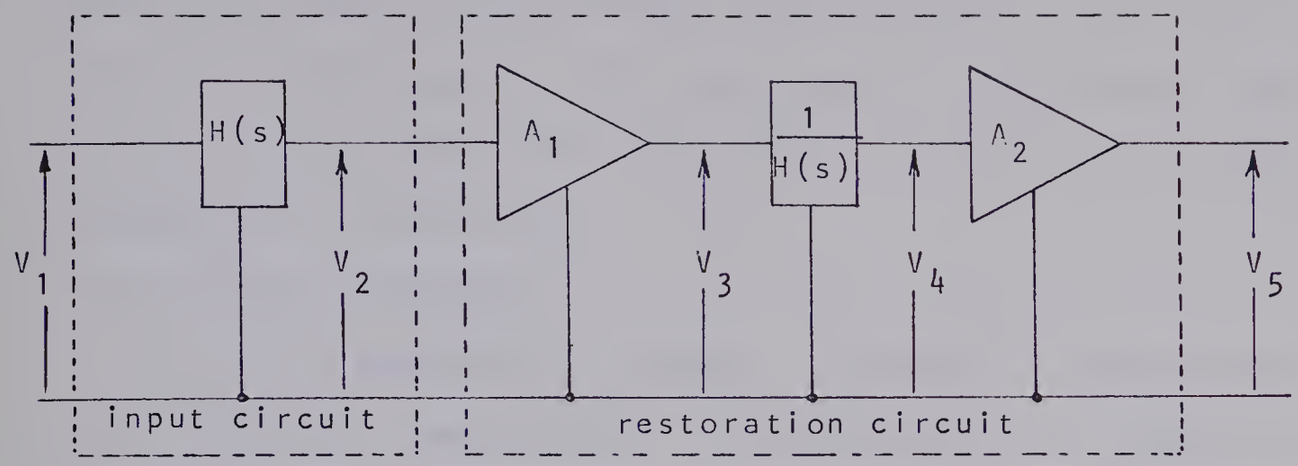

(a)

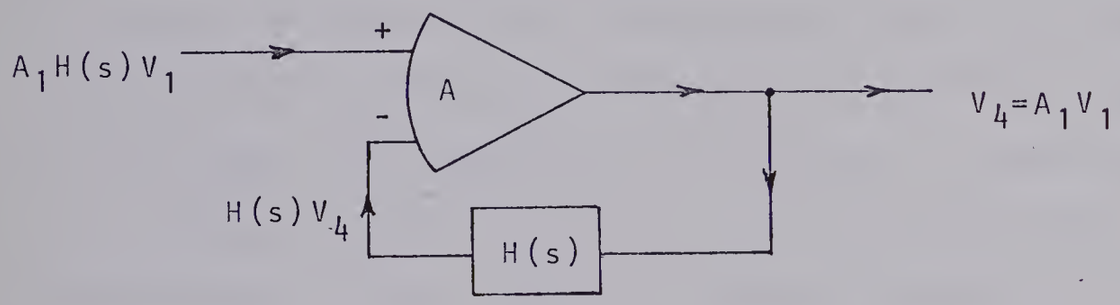

(b)

Figure 1-6
Proposed Scheme of Waveform Restoration

the generated cell potential and V_5 is the restored, undistorted waveform amplified by the factor A_1A_2. V_5 can be fed directly to an oscilloscope or may undergo further amplification before display. Fig. 1-6(b) illustrates how the block 1/H(s) is acheived. The required condition is contained in the following equation:

$$A_1H(s)V_1 - H(s)V_4 = 0$$

This condition can be met with the use of an operational

amplifier characterized by high input impedance and high differential voltage gain. The output of the operational amplifier will be an amplified version of V_1 and the undistorted waveform will be restored.

1.8 Subsequent Analysis

In the analysis to follow, a proposal of an equalization scheme for compensation is presented and its feasibility tested. As part of the initial development, existing models of the microelectrode are presented and used as a basis for establishing a convenient and accurate electrical equivalent of the probe. The majority of this paper is concerned with the mathematical description of the electrode, both from the point of view of its two-port parameters and its voltage transfer function H(s). The latter is useful in establishing the stability of the proposed equalization scheme.

CHAPTER II

THE EQUIVALENT CIRCUIT

2.1 General

The mathematical analysis of any physical, electrical system requires the choice of some equivalent electrical representation of the system. The equivalent circuit is usually chosen to be as simple as the limits of accuracy required will allow. This ensures, hopefully, a possible, if not simple, mathematical analysis of the system yielding the desired design information.

The system of interest in this investigation is the electrolyte-filled capillary microelectrode in its measuring environment. In all previous work, designers have relied on the two-element R-C low-pass network (Figure I-3b) as this system's equivalent circuit. All forms of reducing distortion have been based on this simplified representation. Closer to the problem at hand, Woodbury used network equalization based on this simple model to approximately restore the undistorted waveform.[1] He was quite successful with slow rises of potentials but fast rising potentials reached the display distorted.

The selection of a model in this investigation is based on the following criteria:

1. A more accurate representation of the system than was assumed by previous investigators with regards

to waveform restoration.

2. Possibility of fabrication using thin-film distributed parameter networks.

3. Fabricated circuit of the model should lend itself to a method of continuous equalization should the characteristics of the physical system change.

The remainder of this chapter is devoted to the adoption of an improved model and a mathematical representation of its distributed parameters.

2.2 Adopted Equivalent Circuit

From the considerations of Section 2-1 the following equivalent circuit has been adopted as a more accurate representation of the microelectrode in its measuring environment:

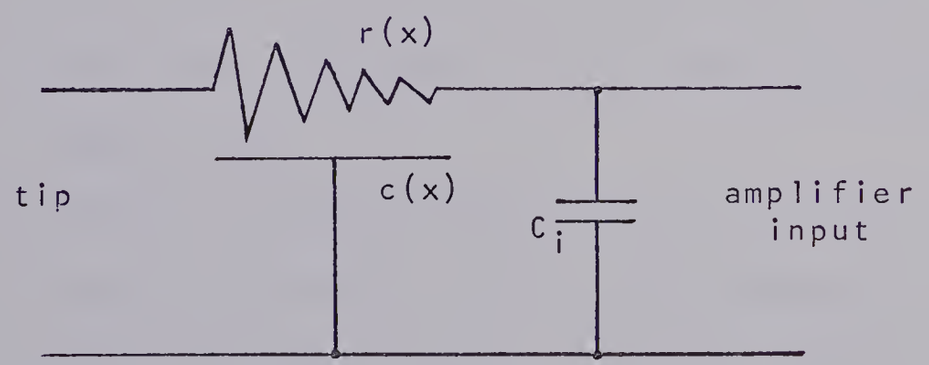

r(x) is resistance variation along the electrode
c(x) is capacitance variation along the electrode
C_i is the amplifier input capacitance

Figure II-1
Adopted Equivalent Circuit

This model is based on Woodbury's consideration that the electrode is equivalent electrically to a continuous R-C transmission line. C_i is included to account for the capacitance contributed to the system by the amplifier and the interconnecting leads.

This equivalent circuit is definitely superior to the two-element model, but essentially consistent with Amatniek's proposal.[1] Due to its simplicity and continuity, the present model should lend itself to thin-film fabrication and some form of continuously monitored equalization.

2-3 Electrode Capacitance Variation

The determination of the capacitance variation along the electrode is based on the following known facts:

1. The depth of Ringer's fluid above the tissue is about 2 mm.
2. Glass is usually either Pyrex or Phoenix.
3. Lumen is normally 2/3 of outer diameter.
4. Ratio of lumen to wall thickness remains constant throughout with the ratio varying less than 5%.

At any particular point of the microelectrode immersed in Ringer's fluid, the electrode has the capacitive properties of a coaxial cylinder. This is illustrated in Fig. II-2. The coaxial cylinder is characterized by the capacitive

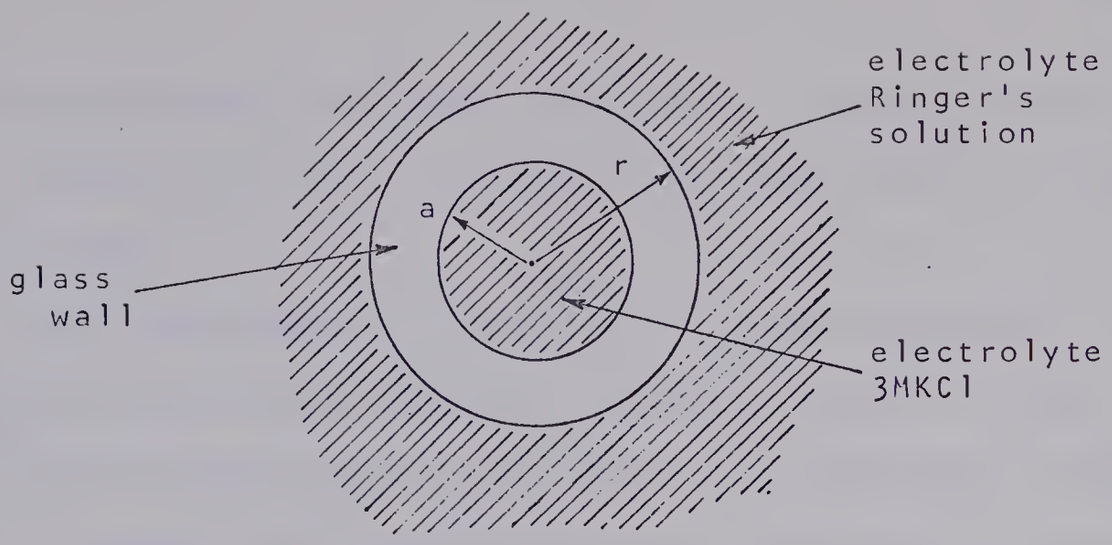

Figure II-2
Electrode Cross-Section

distribution $c(x)=2\pi\varepsilon/\ln(r/a)$, where ε is the dielectric constant of the insulating medium. With the slope of the capillary gradual and the ratio of lumen to outer diameter constant throughout the length, the equation for the capacitance of a coaxial cylinder is applicable to the electrode. This indicates that the distributed capacitance of the electrode will be constant (per unit length). This is in accordance with the assumptions of previous investigators.

2.4 Electrode Resistance Variation

In the determination of the resistance variation along the electrode the following assumptions are made:

1. All electrode resistance is due to the thin column of electrolyte within the capillary.
2. The electrode is conical in form with constant slope in the shank region.
3. Electrolyte resistivity is constant throughout.

These assumptions provide the basis for a mathematical

description of the electrode resistance. The accuracy of this treatment will be sufficient within the limits of the assumed model.

The derivation of the per unit length resistance $r(x)=\frac{dR}{dx}$ of the conical column is based on the well known relationship governing the resistance of a conductor: $R=\rho\frac{L}{A}$.

A geometrical representation of the column is given in Figure II-3a. Aside from the obvious area relationships

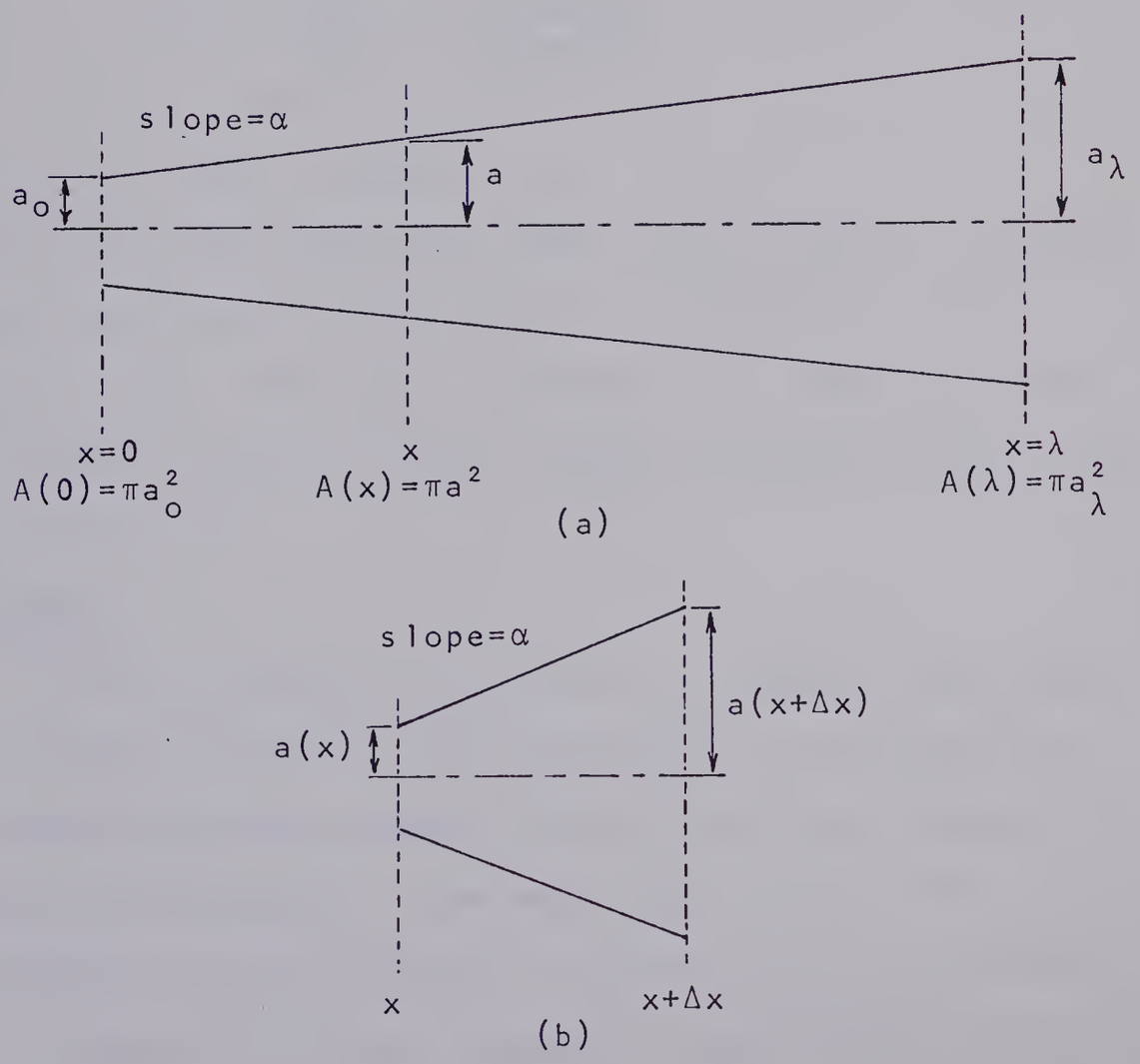

Figure II-3
Geometrical Representation of Electrolyte Column

shown in the diagram, the following equations may be written:

$a(x) = a_o + \alpha x$ radius of column at x

$A(x) = \pi(a_o + \alpha x)^2$ cross-sectional area at x

A differential element of the column is presented in Figure II-3b. For the element:

$$r(x) = \frac{dR}{dx} = \lim_{\Delta x \to 0} \frac{\Delta R}{\Delta x}$$

It can easily be shown that:

$$r(x) = \frac{\rho}{A(x)} = \frac{\rho}{\pi(a_o+\alpha x)^2}$$

(for details consult Appendix I)

The function r(x) above describes the resistance variation of the electrolytic column within the capillary of the microelectrode. The space parameter x is always positive and increases along the axial length of the microelectrode, away from the tip.

2.5 Summary

In this chapter an equivalent circuit of the electrolyte-filled capillary microelectrode in its measuring environment has been adopted, based largely on the work of previous investigators. The model consists of a R-C low-pass distributed parameter network, representing the microelectrode, shunted by a single capacitor representing all capacitive contributions exterior to the electrode. The resistance and capacitance variations of the distributed parameter

network have been derived and are presented as follows:

$$c(x) = c_o \qquad \{2\text{-}1\}$$

$$r(x) = \frac{\rho}{\pi(a_o+\alpha x)^2} \qquad \{2\text{-}2\}$$

CHAPTER III

MATHEMATICAL ANALYSIS

3.1 General

In the analysis to follow, the equivalent circuit of the microelectrode in its measuring environment is divided into two functional blocks. This is illustrated in Figure III-1. This division is convenient for two reasons:

1. It isolates and simplifies the analysis.
2. It constitutes a logical division with respect to some ensuing scheme of continuous equalization, since the elements of each block are subject to independent variation.

Due to the complexity inherent to the analysis of distributed parameter networks, the majority of this chapter is concerned with the analysis of the first functional block. The consideration of the two blocks cascaded results in a description of the complete network.

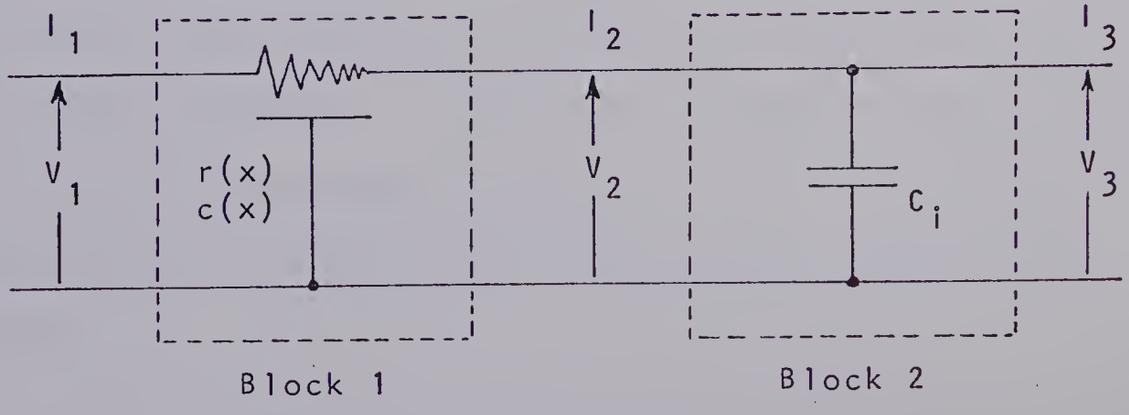

Figure III-1
Microelectrode Equivalent Circuit

In this investigation the goals of the analysis are two-fold:

1. To provide the basis upon which the feasibility of the compensation proposal can be tested.
2. To provide information which may be of interest to investigators concerned with the properties of non-uniform distributed R-C lines.

In the analysis to follow the characterizing partial differential equation for voltage along the line is solved. The resulting product solution is used to resolve the sinusoidal steady-state solutions for both line voltage and current. These solutions are employed to derive the z-parameters of the line. The derived z-parameter matrix contains all the information necessary towards the derivation of any two-port network parameter of interest. A recently evolved method of analysis[30] is used to derive the network function of the system, where H(s) is expressed in terms of a uniformly convergent series of s. The coefficients of this series are used to extract information regarding the line's time domain behavior. The network function H(s) will form the basis for subsequent tests which will be necessary in determining the stability of the proposed compensation scheme.

3.2 Analysis of the Distributed R-C Line

Part I - The Differential Equation

The first functional block of the complete network represents a tapered distributed R-C line with the following resistance and capacitance distributions:

$$c(x) = c_o \qquad \{3\text{-}1\}$$

$$r(x) = \frac{\rho}{\pi(a_o+\alpha x)^2} \qquad \{3\text{-}2\}$$

With the increased interest in microelectronics and integrated circuits, the analysis of distributed parameter networks has received the attention of many investigators[14-31] in recent years.

In the analysis to follow, the traditional approach will be employed. The analysis will be based upon the solution of the line's characterizing differential equation. From the complete solution the sinusoidal steady-state solution is readily derived. The steady-state solution is in turn used to derive any required set of the network's two-port parameters. In this case, the network's z-parameters are presented.

3.2.1 The Differential Equation

Kaufman and Garrett[23] have shown that, if attention is restricted to one dimensional current flow, the general nonuniform distributed R-C line is characterized by a second-order partial differential

equation with variable coefficients. The derivation is presented in Appendix II with the following equations:

$$\frac{\partial^2 v}{\partial x^2} - \frac{1}{r(x)} \frac{dr(x)}{dx} \frac{\partial v}{\partial x} = r(x)\ c(x) \frac{\partial v}{\partial t} \qquad \{3\text{-}3\}$$

$$\frac{\partial^2 i}{\partial x^2} - \frac{1}{c(x)} \frac{dc(x)}{dx} \frac{\partial i}{\partial x} = r(x)\ c(x) \frac{\partial i}{\partial t} \qquad \{3\text{-}4\}$$

Both voltage (v) and current (i) are functions of both time (t) and distance along the line (x). The solution of these equations in closed form for arbitrary r(x) and c(x) has not been found; even the steady-state solution is too complicated.[25] A straight forward solution exists for the uniform line (no taper) while other solutions, if possible, are quite involved. The special case, where the product r(x)c(x) is a constant, has received considerable treatment because of the ease of fabricating such a line.

In this investigation the solution of {3-3} with the resistance and capacitance distributions of {3-1} and {3-2} is of interest. With the substitution of {3-1} and {3-2} :

$$\frac{1}{r(x)} \frac{dr(x)}{dx} = - \frac{2\alpha}{a_o + \alpha x} \qquad \{3\text{-}5\}$$

$$r(x)c(x) = \frac{\rho c_o}{\pi(a_o+\alpha x)^2} \qquad \{3\text{-}6\}$$

Therefore {3-3} becomes:

$$\frac{\partial^2 v}{\partial x^2} + \frac{2}{a_o+\alpha x}\frac{\partial v}{\partial x} = \frac{\rho c_o}{\pi(a_o+\alpha x)^2}\frac{\partial v}{\partial t} \qquad \{3\text{-}7\}$$

This can be written in the form:

$$\frac{\pi}{\rho c_o}(a_o+\alpha x)^2\frac{\partial^2 v(x,t)}{\partial x^2} + \frac{2\pi\alpha}{\rho c_o}(a_o+\alpha x)\frac{\partial v(x,t)}{\partial x} = \frac{\partial v(x,t)}{\partial t} \qquad \{3\text{-}8\}$$

3.2.2 Solution

A solution will be attempted of the form:

$$v(x,t) = T(t)\,X(x) = V(t)\,V(x) \qquad \{3\text{-}9\}$$

Substitution of the trial solution into the equation ({3-8}) and separation of variables results in two separate ordinary differential equations, one with time t as the independent variable and the other with distance x as the independent variable:

$$\frac{\pi}{\rho c_o}(a_o+\alpha x)^2\frac{1}{X}\frac{d^2X}{dx^2} + \frac{2\pi\alpha}{\rho c_o}(a_0+\alpha x)\frac{1}{X}\frac{dX}{dx} = -k^2 \qquad \{3\text{-}10\}$$

$$\frac{1}{T}\frac{dT}{dt} = -k^2 \qquad \{3\text{-}11\}$$

This separation into two ordinary differential equations indicates that a product solution does in fact exist. The parameters k^2 which satisfy the equations and associated boundary conditions are termed eigenvalues

and the resulting functions X(x) and T(t) are termed eigenfunctions. The final solution to an eigenvalue problem may be expressed in series form composed of an infinite number of normal modes.(33)

the solution T(t)

The equation may be expressed as:

$$\frac{dT}{dt} + k^2 T = 0 \qquad \{3\text{-}12\}$$

The solution is easily resolved as:

$$V(t) = T(t) = A\, e^{-k^2 t} \quad ; \quad A = T(t=0^+) \qquad \{3\text{-}13\}$$

the solution X(x)

The equation may be expressed as:

$$(a_o+\alpha x)^2 \frac{d^2X}{dx^2} + 2\alpha(a_o+\alpha x) \frac{dX}{dx} + \frac{\rho c_o}{\pi} k^2 X = 0 \qquad \{3\text{-}14\}$$

This equation has the form of Legendre's Linear Equation and can be reduced to an ordinary differential equation with constant coefficients by using the following transformation(32):

$$e^z = (a_o+\alpha x)$$

The details of the transformation are presented in Appendix III. In the transformed space the equation becomes:

$$\frac{d^2X}{dz^2} + \frac{dX}{dz} + \frac{\rho c_o}{\pi \alpha^2} k^2 X = 0 \quad ; \quad X(z) \leftrightarrow X(x) \qquad \{3\text{-}15\}$$

Assuming a solution of the form $X=e^{\gamma z}$ yields the following characteristic equation:

$$\gamma^2 + \gamma + \frac{\rho c_o}{\pi \alpha^2} k^2 = 0 \qquad \{3\text{-}16\}$$

Solution of this equation yields the characteristic roots:

$$\gamma_{12} = \tfrac{1}{2}(-1 \pm \theta') \qquad \{3\text{-}17\}$$

$$\theta' = \left(1 - 4k^2 \frac{\rho c_o}{\pi \alpha^2}\right)^{\frac{1}{2}} \qquad \{3\text{-}18\}$$

The solution in the z-space takes the form:

$$X(z) = B\, e^{\gamma_1 z} + C\, e^{\gamma_2 z} \qquad \{3\text{-}19\}$$

where B and C are constants dependent on the boundary conditions.

The solution can also be expressed as:

$$X(z) = e^{-\frac{1}{2}z}\left(B\, e^{\frac{1}{2}\theta' z} + C\, e^{-\frac{1}{2}\theta' z}\right) \qquad \{3\text{-}20\}$$

Consider the identities:

$$e^{\frac{1}{2}\theta' z} = \cosh \tfrac{1}{2}\theta' z + \sinh \tfrac{1}{2}\theta' z$$

$$e^{-\frac{1}{2}\theta' z} = \cosh \tfrac{1}{2}\theta' z - \sinh \tfrac{1}{2}\theta' z$$

Using these relationships, equation {3-20} becomes:

$$X(z) = e^{-\frac{1}{2}z}\left(c_1 \sinh \tfrac{1}{2}\theta' z + c_2 \cosh \tfrac{1}{2}\theta' z\right)$$

where: $c_1 = B - C \quad ; \quad c_2 = B + C$

This form of the solution will prove more convenient in the subsequent analysis. Since $e^z = a_o+\alpha x$, the solution in the x-space is:

$$V(x) = X(x) = (a_o+\alpha x)^{-\frac{1}{2}} \left[c_1 \sinh\phi(x) + c_2 \cosh\phi(x) \right]$$

where: $$\phi(x) = \tfrac{1}{2}\theta' \ln(a_o+\alpha x)$$

$$\theta' = \left(1 - 4k^2 \frac{\rho c_o}{\pi \alpha^2}\right)^{\frac{1}{2}}$$

{3-21}

Substituting {3-13} and {3-21} into {3-9} yields a solution {3-22}:

$$v(x,t) = \frac{e^{-k^2 t}}{(a_o+\alpha x)^{\frac{1}{2}}} \left[c_3 \sinh\phi(x) + c_4 \cosh\phi(x)\right] \qquad \{3\text{-}22\}$$

where: $c_3 = A\, c_1 \quad ; \quad c_4 = A\, c_2$

<u>the complete solution</u>

A solution of the line's characterizing differential equation ({3-8}) has been found and is expressed in {3-22}. The general solution may be expressed as:

$$v(x,t) = c_0 + \sum_i X(k_i,x)\, T(k_i,t)$$

Therefore the complete solution to {3-8} may be expressed as:

$$v(x,t) = c_0 + \sum_i \frac{e^{-k_i^2 t}}{(a_o+\alpha x)^{\frac{1}{2}}} \left[c_3 \sinh\phi(x) + c_4 \cosh\phi(x)\right] \qquad \{3\text{-}23\}$$

where c_0, c_3 and c_4 are constants determined by the conditions to which the line is subjected and the values k_i represent the eigenvalues.

3.2.3 Sinusoidal Steady-State Solution

the voltage solution

For the sinusoidal steady-state response:

$$v(x,t) = \text{Re}\left[c_0 + V(x)e^{st}\right] \; ; \; s=j\omega$$

From {3-21} :

$$V(x) = (a_o+\alpha x)^{-\frac{1}{2}}\left[\, c_1 \sinh\phi(x) + c_2 \cosh\phi(x) \,\right]$$

From {3-23} recognize: $s = -k_i^2 = j\omega$

Therefore: $k_i^2 = -j\omega$ {3-24}

The sinusoidal steady-state solution of line voltage is recognized as the space solution {3-21} held to the confines of {3-24}. Therefore, in the sinusoidal steady-state:

$$v(x,t)\Big|_{sss} = V(x) = (a_o+\alpha x)^{-\frac{1}{2}}\left[c_1 \sinh\phi(x) + c_2 \cosh\phi(x)\right]$$

where: $\phi(x) = \frac{1}{2}\theta' \ln(a_o+\alpha x)$

$$\theta' = \left(1 + j\omega\frac{4\rho c_o}{\pi\alpha^2}\right)^{\frac{1}{2}}$$

{3-25}

the current solution:

It has been shown (Appendix II) that the current in the line is related to voltage by:

$$i = -\frac{1}{r(x)}\frac{\partial v}{\partial x} \qquad \begin{matrix} i = i(x,t) \\ v = v(x,t) \end{matrix} \qquad \{3\text{-}26\}$$

For the sinusoidal steady-state response:

$$i(x,t) = \mathrm{Re}\left[I(x)e^{st}\right] \quad ; \quad s=j\omega$$

Therefore:

$$I(x) = -\frac{1}{r(x)}\frac{dV(x)}{dx} \qquad \{3\text{-}27\}$$

Evaluating $\frac{d}{dx}V(x)$:

$$\frac{dV(x)}{dx} = \frac{d}{dx}\left[\frac{c_1}{(a_o+\alpha x)^{\frac{1}{2}}}\sinh\phi(x) + \frac{c_2}{(a_o+\alpha x)^{\frac{1}{2}}}\cosh\phi(x)\right] \qquad \{3\text{-}28\}$$

Expanding the differentiation yields:

$$\frac{dV(x)}{dx} = \frac{\alpha}{2}(a_o+\alpha x)^{-\frac{3}{2}}\left[(c_2\theta'-c_1)\sinh\phi(x) + (c_1\theta'-c_2)\cosh\phi(x)\right]$$

Therefore, in the sinusoidal steady-state:

$$i(x,t)\Big|_{sss} = -\frac{\pi\alpha}{2\rho}(a_o+\alpha x)^{\frac{1}{2}}\left[(c_2\theta'-c_1)\sinh\phi(x) + (c_1\theta'-c_2)\cosh\phi(x)\right]$$

where:

$$\phi(x) = \tfrac{1}{2}\theta'\ln(a_o+\alpha x)$$

$$\theta' = \left(1 + j\omega\frac{4\rho c_o}{\pi\alpha^2}\right)^{\frac{1}{2}} \qquad \{3\text{-}29\}$$

Equations {3-25} and {3-29} represent the sinusoidal steady-state solutions for the line. These equations form the basis for the following development deriving the impedance matrix for the network.

3.2.4 Network z Parameters

In section 3.2.3 the following expressions were derived for the voltage and current sinusoidal steady-state responses:

$$V(x) = (a_o+\alpha x)^{-\frac{1}{2}} \left[c_1 \sinh\phi(x) + c_2 \cosh\phi(x)\right] \qquad \{3\text{-}30\}$$

$$I(x) = -\frac{\pi\alpha}{2\rho}(a_o+\alpha x)^{\frac{1}{2}}\left[(c_2\theta'-c_1)\sinh\phi(x) + (c_1\theta'-c_2)\cosh\phi(x)\right] \qquad \{3\text{-}31\}$$

Consider the following two-port network with the boundary conditions as shown:

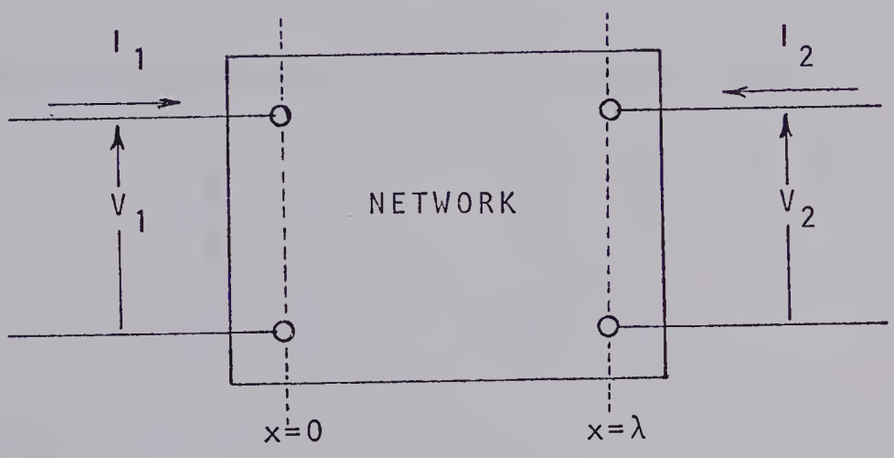

Figure III-2
Two Port Network

With the voltage and current equations governing the network known, the z-parameter matrix can be formed:

$$\begin{bmatrix} V_1 \\ V_2 \end{bmatrix} = \begin{bmatrix} z_{11} & z_{12} \\ z_{21} & z_{22} \end{bmatrix} \begin{bmatrix} I_1 \\ I_2 \end{bmatrix} \qquad \{3\text{-}32\}$$

or

$$V] = [z][I \qquad \{3\text{-}33\}$$

Consider the boundary conditions:

at $x=0$ $\quad V(x)=V_1$ $\qquad$ at $x=\lambda$ $\quad V(x)=V_2$

$\qquad\qquad I(x)=I_1 \qquad\qquad\qquad\qquad -I(x)=I_2$

Substituting these conditions into {3-30} yields:

$$V_1 = V(0) = a_o^{-\frac{1}{2}}\left[c_1 \sinh\phi(0) + c_2 \cosh\phi(0)\right] \qquad \{3\text{-}34\}$$

$$V_2 = V(\lambda) = (a_o+\alpha x)^{-\frac{1}{2}}\left[c_1 \sinh\phi(\lambda) + c_2 \cosh\phi(\lambda)\right] \qquad \{3\text{-}35\}$$

where:

$$\phi(0) = \tfrac{1}{2}\theta' \ln a_o$$

$$\phi(\lambda) = \tfrac{1}{2}\theta' \ln(a_o+\alpha x)$$

Expressing {3-34} and {3-35} in matrix form:

$$\begin{bmatrix} V_1 \\ V_2 \end{bmatrix} = \begin{bmatrix} d_{11} & d_{12} \\ d_{21} & d_{22} \end{bmatrix} \begin{bmatrix} c_1 \\ c_2 \end{bmatrix} \qquad \{3\text{-}36\}$$

In matrix notation:

$$V] = [D][c \qquad \{3\text{-}37\}$$

where:

$$d_{11} = a_o^{-\frac{1}{2}} \sinh \phi(0)$$

$$d_{12} = a_o^{-\frac{1}{2}} \cosh \phi(0)$$

$$d_{21} = (a_o+\alpha\lambda)^{-\frac{1}{2}} \sinh\phi(\lambda) \qquad \{3\text{-}38\}$$

$$d_{22} = (a_o+\alpha\lambda)^{-\frac{1}{2}} \cosh\phi(\lambda)$$

Substituting the boundary conditions into {3-31} yields:

$$I_1 = I(0) = -\frac{\pi\alpha}{2\rho}a_o^{\frac{1}{2}}[(c_2\theta'-c_1)\sinh\phi(0) + (c_1\theta'-c_2)\cosh\phi(0)] \quad \{3\text{-}39\}$$

$$I_2 = I(\lambda) = \frac{\pi\alpha}{2\rho}(a_o+\alpha\lambda)^{\frac{1}{2}}[(c_2\theta'-c_1)\sinh\phi(\lambda) + (c_1\theta'-c_2)\cosh\phi(\lambda)] \quad \{3\text{-}40\}$$

Rearranging {3-39} and {3-40} yields:

$$I_1 = \frac{\pi\alpha}{2\rho}a_o^{\frac{1}{2}}\left[[\sinh\phi(0) - \theta'\cosh\phi(0)]c_1 + [\cosh\phi(0) - \theta'\sinh\phi(0)]c_2\right] \quad \{3\text{-}41\}$$

$$I_2 = -\frac{\pi\alpha}{2\rho}(a_o+\alpha\lambda)^{\frac{1}{2}}\left[[\sinh\phi(\lambda) - \theta'\cosh\phi(\lambda)]c_1 + [\cosh\phi(\lambda) - \theta'\sinh\phi(\lambda)]c_2\right] \quad \{3\text{-}42\}$$

Expressing {3-41} and {3-42} in matrix form:

$$\begin{bmatrix} I_1 \\ I_2 \end{bmatrix} = \begin{bmatrix} a_{11} & a_{12} \\ a_{21} & a_{22} \end{bmatrix} \begin{bmatrix} c_1 \\ c_2 \end{bmatrix} \quad \{3\text{-}43\}$$

where:

$$a_{11} = \frac{\pi\alpha}{2\rho}\,a_o^{\frac{1}{2}}\,[\sinh\phi(0) - \theta'\cosh\phi(0)]$$

$$a_{12} = \frac{\pi\alpha}{2\rho}\,a_o^{\frac{1}{2}}\,[\cosh\phi(0) - \theta'\sinh\phi(0)]$$

$$a_{21} = -\frac{\pi\alpha}{2\rho}\,(a_o+\alpha\lambda)^{\frac{1}{2}}\,[\sinh\phi(\lambda) - \theta'\cosh\phi(\lambda)]$$

$$a_{22} = -\frac{\pi\alpha}{2\rho}\,(a_o+\alpha\lambda)^{\frac{1}{2}}\,[\cosh\phi(\lambda) - \theta'\sinh\phi(\lambda)] \quad \{3\text{-}44\}$$

In matrix notation: $I] = [A][c$ {3-45}

Consider the following matrix development:

$$V] = [Z][I$$

$$V] = [D][c$$

$$I] = [A][c$$

$$\text{now} \quad [A]^{-1} I] = [A]^{-1}[A][c = [c$$

$$\text{let} \quad [B] = [A]^{-1}$$

$$\text{therefore} \quad c] = [B][I$$

$$\text{and} \quad V] = [D][B][I$$

$$\text{therefore} \quad [Z] = [D][B] \qquad \{3\text{-}46\}$$

The next step in the development will be the formation of matrix [B] which is the inverse of matrix [A]. For the 2 x 2 array:[33]

$$[B] = [A]^{-1} = \frac{1}{\det[A]} \begin{bmatrix} a_{22} & -a_{12} \\ -a_{21} & a_{11} \end{bmatrix} \qquad \{3\text{-}47\}$$

where: $\det[A] = a_{11}a_{22} - a_{12}a_{21}$

Evaluating det [A]:

$$a_{11}a_{22} = -\left(\frac{\pi\alpha}{2\rho}\right)^2 [a_o(a_o+\alpha\lambda)]^{\frac{1}{2}} \Big[\sinh\phi(0)\cosh\phi(\lambda) + \theta'^2\sinh\phi(\lambda)\cosh\phi(0) - \theta'\cosh\phi(0)\cosh\phi(\lambda) - \theta'\sinh\phi(0)\sinh\phi(\lambda)\Big]$$

$$a_{12}a_{21} = -\left(\frac{\pi\alpha}{2\rho}\right)^2 \left[a_o(a_o+\alpha\lambda)\right]^{\frac{1}{2}} \Big[\cosh\phi(0)\sinh\phi(\lambda) + \theta'^2\sinh\phi(0)\cosh\phi(\lambda) - \theta'\cosh\phi(0)\cosh\phi(\lambda) - \theta'\sinh\phi(0)\sinh\phi(\lambda)\Big]$$

$$\det[A] = -\left(\frac{\pi\alpha}{2\rho}\right)^2 \left[a_o(a_o+\alpha\lambda)\right]^{\frac{1}{2}} (1-\theta'^2) \cdots\cdots \cdots [\sinh\phi(0)\cosh\phi(\lambda) - \cosh\phi(0)\sinh\phi(\lambda)] \quad \{3\text{-}48\}$$

Using the identity:

$$\sinh(x-y) = \sinh x \cosh y - \cosh x \sinh y$$

Equation {3-48} becomes:

$$\det[A] = -\left(\frac{\pi\alpha}{2\rho}\right)^2 \left[a_o(a_o+\alpha\lambda)\right]^{\frac{1}{2}} (1-\theta'^2)\sinh[\phi(0)-\phi(\lambda)] \quad \{3\text{-}49\}$$

where:

$$\phi(0) - \phi(\lambda) = \tfrac{1}{2}\theta' \ln\left(\frac{a_o}{a_o+\alpha\lambda}\right)$$

Note: From Appendix IV

$\det[A] = 0$ if, and only if $\omega = 0$

therefore $[B]$ is defined for all conditions except $\omega = 0$.

Using {3-44}, {3-47} and {3-49} yields the parameters of matrix [B]:

$$b_{11} = \frac{a_{22}}{\det[A]} = \frac{2\rho}{\pi\alpha} \frac{\cosh\phi(\lambda) - \theta'\sinh\phi(\lambda)}{a_o^{\frac{1}{2}}(1-\theta'^2)\sinh[\phi(0)-\phi(\lambda)]}$$

$$b_{12} = \frac{-a_{12}}{\det[A]} = \frac{-2\rho}{\pi\alpha} \frac{\theta'\sinh\phi(0) - \cosh\phi(0)}{(a_o+\alpha\lambda)^{\frac{1}{2}}(1-\theta'^2)\sinh[\phi(0)-\phi(\lambda)]}$$

$$b_{21} = \frac{-a_{21}}{\det[A]} = \frac{2\rho}{\pi\alpha} \frac{\theta'\cosh\phi(\lambda) - \sinh\phi(\lambda)}{a_o^{\frac{1}{2}}(1-\theta'^2)\sinh[\phi(0)-\phi(\lambda)]}$$

$$b_{22} = \frac{a_{11}}{\det[A]} = \frac{-2\rho}{\pi\alpha} \frac{\sinh\phi(0) - \theta'\cosh\phi(0)}{(a_o+\alpha\lambda)^{\frac{1}{2}}(1-\theta'^2)\sinh[\phi(0)-\phi(\lambda)]}$$

{3-50}

Now recall: $[Z] = [D][B]$ {3-51}

or:

$$\begin{bmatrix} z_{11} & z_{12} \\ z_{21} & z_{22} \end{bmatrix} = \begin{bmatrix} d_{11} & d_{12} \\ d_{21} & d_{22} \end{bmatrix} \begin{bmatrix} b_{11} & b_{12} \\ b_{21} & b_{22} \end{bmatrix} \quad \{3\text{-}52\}$$

Expanding the product yields:

$$\begin{aligned} z_{11} &= d_{11}b_{11} + d_{12}b_{21} \\ z_{12} &= d_{11}b_{12} + d_{12}b_{22} \\ z_{21} &= d_{21}b_{11} + d_{22}b_{21} \\ z_{22} &= d_{21}b_{12} + d_{22}b_{22} \end{aligned} \quad \{3\text{-}53\}$$

Using the identities:

$$\sinh(x - y) = \sinh x \cosh y - \cosh x \sinh y$$

$$\cosh(x - y) = \cosh x \cosh y - \sinh x \sinh y$$

and some algebraic manipulations, the following z-parameters are resolved:

$$z_{11} = \frac{2\rho}{\pi\alpha a_o(1-\theta'^2)}\left[1 + \frac{\theta'}{\tanh[\phi(0)-\phi(\lambda)]}\right]$$

$$z_{12} = z_{21} = \frac{2\rho}{\pi\alpha[a_o(a_o+\alpha\lambda)]^{\frac{1}{2}}(1-\theta'^2)}\left[\frac{\theta'}{\sinh[\phi(0)-\phi(\lambda)]}\right] \quad \{3\text{-}54\}$$

$$z_{22} = \frac{-2\rho}{\pi\alpha(a_o+\alpha\lambda)(1-\theta'^2)}\left[1 - \frac{\theta'}{\tanh[\phi(0)-\phi(\lambda)]}\right]$$

The expressions for the z-parameters in {3-54} can be altered to a more convenient form by making use of the following relationships:

$$\theta' = \frac{2a_o}{\pi\alpha}\theta \quad \text{where:} \quad \theta = \left[\frac{\alpha^2\lambda^2}{4a_o^2} + j\omega\frac{\rho c_o \lambda^2}{\pi a_o^2}\right]^{\frac{1}{2}}$$

$$\tanh(-x) = -\tanh x$$

$$\phi(\lambda) - \phi(0) = \tfrac{1}{2}\theta' \ln\left(1 + \frac{\alpha\lambda}{a_o}\right)$$

$$= \frac{a_o}{\alpha\lambda}\theta \ln\left(1 + \frac{\alpha\lambda}{a_o}\right)$$

$$1 - \theta'^2 = -j\omega\frac{4\rho c_o}{\pi\alpha^2}$$

The final form of the z-parameters is presented as follows:

$$z_{11} = \frac{1}{j\omega c_o \lambda}\left[\frac{\theta}{\tanh\left[\frac{a_o}{\alpha\lambda}\theta \ln\left(1+\frac{\alpha\lambda}{a_o}\right)\right]} - \frac{\alpha\lambda}{2a_o}\right] \qquad \{3\text{-}55\}$$

$$z_{12} = z_{21} = \frac{1}{j\omega c_o \lambda\left(1+\frac{\alpha\lambda}{a_o}\right)^{\frac{1}{2}}} \frac{\theta}{\sinh\left[\frac{a_o}{\alpha\lambda}\theta \ln\left(1+\frac{\alpha\lambda}{a_o}\right)\right]} \qquad \{3\text{-}56\}$$

$$z_{22} = \frac{1}{j\omega c_o \lambda\left(1+\frac{\alpha\lambda}{a_o}\right)}\left[\frac{\theta}{\tanh\left[\frac{a_o}{\alpha\lambda}\theta \ln\left(1+\frac{\alpha\lambda}{a_o}\right)\right]} + \frac{\alpha\lambda}{2a_o}\right] \qquad \{3\text{-}57\}$$

Let: $$f(\alpha) = \frac{a_o}{\alpha\lambda} \ln\left(1 + \frac{\alpha\lambda}{a_o}\right) \qquad \{3\text{-}58\}$$

In matrix form: $V] = [Z][I$

$$\begin{bmatrix} V_1 \\ V_2 \end{bmatrix} = \frac{1}{j\omega c_o \lambda}\begin{bmatrix} \frac{\theta}{\tanh f(\alpha)\theta} - \frac{\alpha\lambda}{2a_o} & \frac{1}{\left(1+\frac{\alpha\lambda}{a_o}\right)^{\frac{1}{2}}} \frac{\theta}{\sinh f(\alpha)\theta} \\ \frac{1}{\left(1+\frac{\alpha\lambda}{a_o}\right)^{\frac{1}{2}}} \frac{\theta}{\sinh f(\alpha)\theta} & \frac{1}{1+\frac{\alpha\lambda}{a_o}}\left[\frac{\theta}{\tanh f(\alpha)\theta} + \frac{\alpha\lambda}{2a_o}\right] \end{bmatrix} \begin{bmatrix} I_1 \\ I_2 \end{bmatrix}$$

$\{3\text{-}59\}$

In the limit, as α approaches zero:

$$f(\alpha) \rightarrow\rightarrow 1$$

$$\theta \rightarrow\rightarrow \left[j\omega \frac{\rho c_o \lambda^2}{\pi a_o^2}\right]^{\frac{1}{2}}$$

and the z-parameters approach those derived by Castro and Happ[16] for a distributed R-C network with no taper (a uniform line).

With the derivation of the network's z-parameters, these can be used in the subsequent derivation of any set of network parameters of interest.[33] For example, the hybrid or h-parameters may be derived on the following basis:

$$\begin{bmatrix} h_{11} & h_{12} \\ h_{21} & h_{22} \end{bmatrix} = \begin{bmatrix} \frac{\det Z}{z_{22}} & \frac{z_{12}}{z_{22}} \\ \frac{-z_{21}}{z_{22}} & \frac{1}{z_{22}} \end{bmatrix}$$

3.3 Analysis of the Distributed R-C Line

Part II - Network Function H(s)

3.3.1 Introduction

In 1965, Protonotarios and Wing[30] presented a significant contribution to the analysis of non-uniform distributed R-C lines. Their treatment circumvents the difficulties associated with the solution of the governing differential equation and provides a simplified method of deriving the voltage transfer network function H(s). The network function H(s) is extremely useful in network analysis and provides information regarding the time domain behavior of the line.[14]

In their approach, the distributed network is considered as a chain of cascaded two-ports with infinitesmal lumped elements. The ABCD parameters are derived for a single infinitesmal section and the product of n elemental transmission matrices, taken in the limit as $n \to \infty$, yields the transmission parameters of the whole line. The resulting parameters consist of uniformly convergent series which are entire functions of s. A summary of the results is presented in Appendix V.

3.3.2 The Network Function H(s)

The network function H(s) can be derived directly from the transmission parameter A(s) which is defined as follows:

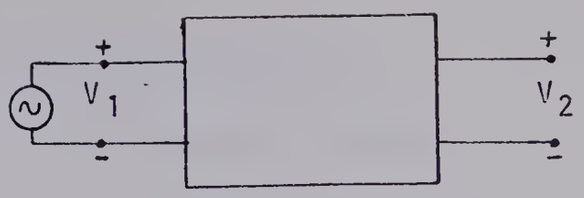

$$A = \left.\frac{V_1}{V_2}\right|_{I_2=0}$$

A is the inverse of the voltage transfer function from port 1 to port 2 with port 2 open-circuited.

Figure III-3
Transmission Parameter A

For considerations regarding an open-circuited R-C line, H(s) can be simply defined as follows:

$$H(s) = \frac{1}{A(s)}$$

3.3.3 Transmission Parameter A(s)

From Appendix V:

$$A(s) = 1 + \sum_{n=1}^{\infty} a_n s^n \qquad \{3\text{-}60\}$$

where:

$$a_n = \int_0^{\lambda} c(x_{2n}) \int_0^{x_{2n}} r(x_{2n-1}) \int_0^{x_{2n-1}} c(x_{2n-2}) \cdots \qquad \{3\text{-}61\}$$

$$\cdots \int_0^{x_3} c(x_2) \int_0^{x_2} r(x_1)\, dx_1\, dx_2 \cdots dx_{2n}$$

For the network of interest, from {2-1} and {2-2}:

$$c(x) = c_o \qquad \{3\text{-}62\}$$

$$r(x) = \frac{\rho}{\pi(a_o+\alpha x)^2} \qquad \{3\text{-}63\}$$

Equations {3-61}, {3-62} and {3-63} are now employed to derive the coefficients a_1, a_2 and a_3.

evaluation of a_1:

From equation {3-61}:

$$a_1 = \int_0^{\lambda} c(x_2) \int_0^{x_2} r(x_1)\, dx_1\, dx_2$$

$$= \int_0^{\lambda} c(x) \int_0^{x} r(y)\, dy\, dx \qquad \{3\text{-}64\}$$

Substitution of equations {3-62} and {3-63} yields:

$$a_1 = \int_0^{\lambda} c_o \int_0^{x} \frac{\rho}{\pi(a_o+\alpha y)^2}\, dy\, dx$$

Now:

$$\int_0^{x} \frac{\rho\, dy}{\pi(a_o+\alpha y)^2} = \frac{\rho}{\pi a_o} \frac{x}{(a_o+\alpha x)}$$

Therefore:

$$a_1 = \frac{\rho c_o}{\pi a_o} \int_0^{x} \frac{x\, dx}{a_o+\alpha x} = \frac{\rho c_o}{\pi\alpha} \left[\frac{\lambda}{a_o} - \frac{1}{\alpha} \ln\left(1+\frac{\alpha\lambda}{a_o}\right) \right] \qquad \{3\text{-}65\}$$

For $\lambda = y$:

$$a_1(y) = \frac{\rho c_o}{\pi\alpha} \left[\frac{y}{a_o} - \frac{1}{\alpha} \ln\left(1+\frac{\alpha y}{a_o}\right) \right] \qquad \{3\text{-}66\}$$

The function $a_1(y)$ above will prove useful in the evaluation of the next coefficient a_2. Generally, the integrations to follow are straight forward but lengthy. For the sake of brevity only the outlining steps are given.

evaluation of a_2:

From {3-61}:

$$a_2 = \int_0^{\lambda} c(x_4) \int_0^{x_4} r(x_3) \int_0^{x_3} c(x_2) \int_0^{x_2} r(x_1)\, dx_1 dx_2 dx_3 dx_4$$

A change in the bases results in:

$$a_2 = \int_0^{\lambda} c(x) \int_0^{x} r(y) \int_0^{y} c(u) \int_0^{u} r(v)\, dv\, du\, dy\, dx \qquad \{3\text{-}67\}$$

From equation {3-64} and {3-66}, recognize:

$$\int_0^{y} c(u) \int_0^{u} r(v)\, dv\, du = a_1(y)$$

Therefore:

$$a_2 = \int_0^{\lambda} c(x) \int_0^{x} r(y) a_1(y)\, dy\, dx \qquad \{3\text{-}68\}$$

Designate:

$$f(x) = \int_0^{x} r(y) a_1(y)\, dy \qquad \{3\text{-}69\}$$

Substituting {3-69} into {3-68} yields:

$$a_2 = \int_0^{\lambda} c(x) f(x)\, dx \qquad \{3\text{-}70\}$$

From {3-63} and {3-66}:

$$r(y) a_1(y) = \frac{\rho^2 c_o}{\pi^2 \alpha} \left[\frac{1}{a_o} \frac{y}{(a_o+\alpha y)^2} - \frac{1}{\alpha a_o^2} \frac{\ln(1+\frac{\alpha y}{a_o})}{(1+\frac{\alpha y}{a_o})^2} \right]$$

Completing the integration in {3-69} yields:

$$f(x) = \frac{\rho^2 c_o}{\pi^2 \alpha^3 a_o}\left[\frac{\ln(1+\frac{\alpha x}{a_o})}{(1+\frac{\alpha x}{a_o})} + \ln(1+\frac{\alpha x}{a_o}) - \frac{2\alpha x}{a_o+\alpha x}\right] \quad \{3\text{-}71\}$$

Finally, using {3-71} and completing the integration in {3-70} yields:

$$a_2 = \frac{\rho^2 c_o^2}{\pi^2 \alpha^2}\left[\frac{1}{2\alpha^2}\ln^2(1+\frac{\alpha\lambda}{a_o}) + \frac{1}{\alpha^2}(3+\frac{\alpha\lambda}{a_o})\ln(1+\frac{\alpha\lambda}{a_o}) - \frac{3\lambda}{\alpha a_o}\right] \quad \{3\text{-}72\}$$

The substitution of y for λ in equation {3-72} yields the function $a_2(y)$ which will be useful in evaluating a_3:

$$a_2(y) = \frac{\rho^2 c_o^2}{\pi^2 \alpha^2}\left[\frac{1}{2\alpha^2}\ln^2(1+\frac{\alpha y}{a_o}) + \frac{1}{\alpha^2}(3+\frac{\alpha y}{a_o})\ln(1+\frac{\alpha y}{a_o}) - \frac{3y}{a_o\alpha}\right] \quad \{3\text{-}73\}$$

evaluation of a_3:

From {3-61}:

$$a_3 = \int_0^{\lambda} c(x_6) \int_0^{x_6} r(x_5) \int_0^{x_5} c(x_4) \int_0^{x_4} r(x_3) \cdots\cdots \cdots\cdots \int_0^{x_3} c(x_2) \int_0^{x_2} r(x_1)\, dx_1 dx_2 \cdots\cdots dx_6$$

A change in bases results in:

$$a_3 = \int_0^{\lambda} c(x) \int_0^{x} r(y) \int_0^{y} c(u) \int_0^{u} r(v) \cdots\cdots\cdots \cdots\cdots \int_0^{v} c(g) \int_0^{g} r(h)\, dh\, dg\, dv\, du\, dy\, dx \quad \{3\text{-}74\}$$

From {3-67} and {3-73} recognize:

$$\int_0^y c(u) \int_0^u r(v) \int_0^v c(g) \int_0^g r(h)\,dh\,dg\,dv\,du = a_2(y)$$

Therefore:

$$a_3 = \int_0^\lambda c(x) \int_0^x r(y)a_2(y)\,dy\,dx \qquad \{3\text{-}75\}$$

Designate:

$$g(x) = \int_0^x r(y)a_2(y)\,dy \qquad \{3\text{-}76\}$$

Substituting {3-76} into {3-75} yields:

$$a_3 = \int_0^\lambda c(x)g(x)\,dx \qquad \{3\text{-}77\}$$

From {3-63} and {3-72}:

$$r(y)a_2(y) = \frac{\rho^3 c_o^2}{\pi^3\alpha^2}\left[\frac{1}{2\alpha^2 a_o^2}\frac{\ln^2(1+\frac{\alpha y}{a_o})}{(1+\frac{\alpha y}{a_o})^2} + \frac{3}{\alpha^2 a_o^2}\frac{\ln(1+\frac{\alpha y}{a_o})}{(1+\frac{\alpha y}{a_o})^2} + \frac{y}{\alpha a_o^3}\frac{\ln(1+\frac{\alpha y}{a_o})}{(1+\frac{\alpha y}{a_o})^2} - \frac{3}{\alpha a_o^3}\frac{y}{(1+\frac{\alpha y}{a_o})^2}\right]$$

Completing the integration in {3-76} yields:

$$g(x) = \frac{\rho^3 c_o^2}{\pi^3\alpha^5 a_o}\left[\tfrac{1}{2}\ln^2(1+\frac{\alpha x}{a_o}) - \tfrac{1}{2}\frac{\ln^2(1+\frac{\alpha x}{a_o})}{(1+\frac{\alpha x}{a_o})} - 3\frac{\ln(1+\frac{\alpha x}{a_o})}{(1+\frac{\alpha x}{a_o})} - 3\ln(1+\frac{\alpha x}{a_o}) + \frac{6}{a_o}\frac{\alpha x}{1+\frac{\alpha x}{a_o}}\right] \qquad \{3\text{-}78\}$$

Finally, using {3-78} and completing the integration in {3-77} yields:

$$a_3 = \frac{\rho^3 c_o^3}{\pi^3 \alpha^6} \left[-\frac{1}{6} \ln^3\left(1+\frac{\alpha\lambda}{a_o}\right) + \frac{1}{2} \left(1+\frac{\alpha\lambda}{a_o}\right) \ln^2\left(1+\frac{\alpha\lambda}{a_o}\right) \right.$$
$$- \frac{3}{2} \ln^2\left(1+\frac{\alpha\lambda}{a_o}\right) - 4 \left(1+\frac{\alpha\lambda}{a_o}\right) \ln\left(1+\frac{\alpha\lambda}{a_o}\right)$$
$$\left. - 6 \ln\left(1+\frac{\alpha\lambda}{a_o}\right) + 9 \frac{\alpha\lambda}{a_o} \right] \qquad \{3\text{-}79\}$$

Note: The series is terminated at three coefficients at the discretion of the author. It is felt that sufficient accuracy is attained at this point and any extension of the analysis will gain very little in overall accuracy.

3.4 Extension of the Analysis to Yield the Network Function of the Complete Equivalent

3.4.1 General

In the preceding analysis the methods of Protonotarios and Wing were employed in deriving the network function of the distributed R-C network. Since the complete equivalent consists of the R-C network shunted by the capacitance C_i an extension of the analysis is necessary.

In the analysis to follow, modified transmission parameters are derived in terms of the transmission parameters of the two components of the complete equivalent.

3.4.2 The Modified Transmission Parameters

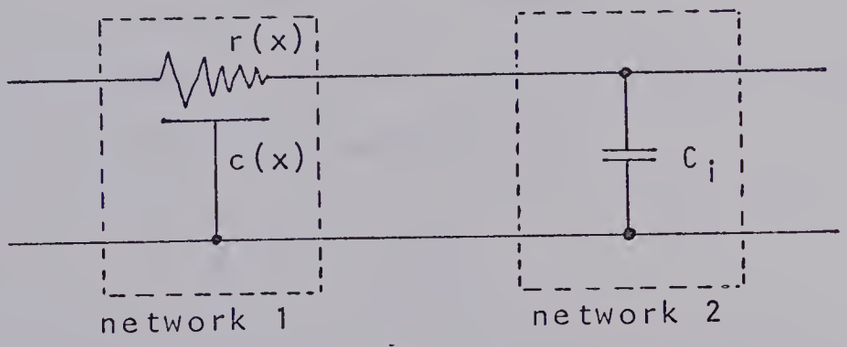

Figure III-1
The Complete Equivalent

Let the transmission parameter matrix of network 1 be:

$$\begin{bmatrix} A_1 & B_1 \\ C_1 & D_1 \end{bmatrix}$$

and let the transmission parameter matrix of network 2 be:

$$\begin{bmatrix} A_2 & B_2 \\ C_2 & D_2 \end{bmatrix} = \begin{bmatrix} 1 & 0 \\ sC_i & 1 \end{bmatrix}$$

The transmission parameter matrix of the system will be equal to the matrix product of the transmission parameter matrices of the equivalent's two cascaded components:

$$\begin{bmatrix} A' & B' \\ C' & D' \end{bmatrix} = \begin{bmatrix} A_1 & B_1 \\ C_1 & D_1 \end{bmatrix} \cdot \begin{bmatrix} 1 & 0 \\ sC_i & 1 \end{bmatrix} = \begin{bmatrix} A_1+sC_iB_1 & B_1 \\ C_1+sC_iD_1 & D_1 \end{bmatrix} \quad \{3\text{-}80\}$$

Of primary interest is the transmission parameter A' where:

$$A' = A_1 + sC_iB_1 \quad \{3\text{-}81\}$$

and the network voltage transfer function of the complete equivalent is defined as:

$$H'(s) = \frac{1}{A'(s)} \quad \{3\text{-}82\}$$

From equation {3-81} it is obvious that an evaluation of A'(s) necessitates the derivation of the transmission parameter $B_1(s)$.

From Appendix V:

$$B_1(s) = \int_0^{\lambda} r(x)\,dx + \sum_{n=1}^{\infty} b_n s^n \quad \{3\text{-}83\}$$

where:

$$b_n = \int_0^{\lambda} r(x_{2n+1}) \int_0^{x_{2n+1}} c(x_{2n}) \int_0^{x_{2n}} r(x_{2n-1}) \cdots \cdots \int_0^{x_3} c(x_2) \int_0^{x_2} r(x_1)\, dx_1 dx_2 \cdots dx_{2n+1} \quad \{3\text{-}84\}$$

As before we have:

$$r(x) = \frac{\rho}{\pi(a_o+\alpha x)^2} \quad ; \quad c(x) = c_o$$

Let:

$$b_o = \int_0^{\lambda} r(x)\, dx \quad \{3\text{-}85\}$$

evaluation of b_o:

$$b_o = \int_0^{\lambda} \frac{\rho\, dx}{\pi(a_o+\alpha x)^2} = \frac{\rho\lambda}{\pi a_o^2 (1+\frac{\alpha\lambda}{a_o})} \quad \{3\text{-}86\}$$

evaluation of b_1:

From {3-84}:

$$b_1 = \int_0^{\lambda} r(x_3) \int_0^{x_3} c(x_2) \int_0^{x_2} r(x_1)\, dx_1\, dx_2\, dx_3$$

A change in bases results in:

$$b_1 = \int_0^{\lambda} r(x) \int_0^{x} c(y) \int_0^{y} r(u)\, du\, dy\, dx \quad \{3\text{-}87\}$$

From {3-85} recognize:

$$\int_0^{y} r(u)\, du = b_o(y)$$

Therefore:

$$b_1 = \int_0^{\lambda} r(x) \int_0^{x} c(y) b_o(y)\, dy\, dx \quad \{3\text{-}88\}$$

Designate:

$$f(x) = \int_0^x c(y)b_o(y)\,dy \qquad \{3\text{-}89\}$$

Substituting {3-89} into {3-88} yields:

$$b_1 = \int_0^\lambda r(x)f(x)\,dx \qquad \{3\text{-}90\}$$

From {3-63} and {3-86}:

$$c(y)b_o(y) = \frac{\rho c_o}{\pi a_o^2}\,\frac{y}{(1+\frac{\alpha y}{a_o})} \qquad \{3\text{-}91\}$$

Completing the integration in {3-89} yields:

$$f(x) = \frac{\rho c_o}{\pi\alpha^2}\left[\frac{\alpha x}{a_o} - \ln(1+\frac{\alpha x}{a_o})\right] \qquad \{3\text{-}92\}$$

Therefore, from {3-63} and {3-92}:

$$r(x)f(x) = \frac{\rho^2 c_o}{\pi^2\alpha^2}\left[\frac{\alpha x}{a_o(a_o+\alpha x)^2} - \frac{\ln(1+\frac{\alpha x}{a_o})}{(a_o+\alpha x)^2}\right] \qquad \{3\text{-}93\}$$

Finally, using {3-93} and completing the integration in {3-90} yields:

$$b_1 = \frac{\rho^2 c_o}{\pi^2\alpha^3 a_o}\left[\ln(1+\frac{\alpha\lambda}{a_o}) + \frac{\ln(1+\frac{\alpha\lambda}{a_o})}{(1+\frac{\alpha\lambda}{a_o})} - 2\,\frac{\alpha\lambda/a_o}{(1+\frac{\alpha\lambda}{a_o})}\right] \qquad \{3\text{-}94\}$$

The substitution of y for λ in the above equation gives the function $b_1(y)$ which will be useful in the evaluation of b_2:

$$b_1(y) = \frac{\rho^2 c_o}{\pi^2\alpha^3 a_o}\left[\ln(1+\frac{\alpha y}{a_o}) + \frac{\ln(1+\frac{\alpha y}{a_o})}{(1+\frac{\alpha y}{a_o})} - 2\,\frac{\alpha y/a_o}{(1+\frac{\alpha y}{a_o})}\right] \qquad \{3\text{-}95\}$$

evaluation of b_2:

From {3-84}:

$$b_2 = \int_0^{\lambda} r(x_5) \int_0^{x_5} c(x_4) \int_0^{x_4} r(x_3) \int_0^{x_3} c(x_2) \int_0^{x_2} r(x_1) \cdots \cdots\cdots\cdots\cdots dx_1\, dx_2\, dx_3\, dx_4\, dx_5$$

A change in the bases results in:

$$b_2 = \int_0^{\lambda} r(x) \int_0^{x} c(y) \int_0^{y} r(u) \int_0^{u} c(v) \int_0^{v} r(t)\, dt\, dv \cdots dx \quad \{3\text{-}96\}$$

From {3-95} recognize:

$$\int_0^{y} r(u) \int_0^{u} c(v) \int_0^{v} r(t)\, dt\, dv\, du = b_1(y)$$

Therefore:

$$b_2 = \int_0^{\lambda} r(x) \int_0^{x} c(y) b_1(y)\, dy\, dx \quad \{3\text{-}97\}$$

Designate:

$$g(x) = \int_0^{x} c(y) b_1(y)\, dy \quad \{3\text{-}98\}$$

Substituting {3-98} into {3-97} yields:

$$b_2 = \int_0^{\lambda} r(x) g(x)\, dx \quad \{3\text{-}99\}$$

From {3-62} and {3-95}:

$$c(y) b_1(y) = \frac{\rho^2 c_o^2}{\pi^2 a_o \alpha^3} \left[\ln\left(1+\frac{\alpha y}{a_o}\right) + \frac{\ln\left(1+\frac{\alpha y}{a_o}\right)}{\left(1+\frac{\alpha y}{a_o}\right)} - 2\frac{\alpha y / a_o}{\left(1+\frac{\alpha y}{a_o}\right)} \right] \quad \{3\text{-}100\}$$

Completing the integration in {3-98} yields:

$$g(x) = \frac{\rho^2 c_o^2}{\pi^2 \alpha^4} \left[\frac{1}{2} \ln^2\left(1+\frac{\alpha x}{a_o}\right) + \left(1+\frac{\alpha x}{a_o}\right) \ln\left(1+\frac{\alpha x}{a_o}\right) + 2\ln\left(1+\frac{\alpha x}{a_o}\right) - 3\frac{\alpha x}{a_o} \right] \qquad \{3\text{-}101\}$$

Therefore, from {3-63} and {3-101}:

$$r(x)g(x) = \frac{\rho^3 c_o^2}{\pi^3 \alpha^4 a_o^2} \left[\frac{1}{2} \frac{\ln^2\left(1+\frac{\alpha x}{a_o}\right)}{\left(1+\frac{\alpha x}{a_o}\right)^2} + \frac{\ln\left(1+\frac{\alpha x}{a_o}\right)}{\left(1+\frac{\alpha x}{a_o}\right)} + 2\frac{\ln\left(1+\frac{\alpha x}{a_o}\right)}{\left(1+\frac{\alpha x}{a_o}\right)^2} - 3\frac{\alpha x/a_o}{\left(1+\frac{\alpha x}{a_o}\right)^2} \right] \qquad \{3\text{-}102\}$$

Finally, using {3-102} and completing the integration in {3-99} yields:

$$b_2 = \frac{\rho^3 c_o^2}{\pi^3 \alpha^5 a_o} \left[\frac{1}{2} \ln^2\left(1+\frac{\alpha\lambda}{a_o}\right) - \frac{1}{2} \frac{\ln^2\left(1+\frac{\alpha\lambda}{a_o}\right)}{\left(1+\frac{\alpha\lambda}{a_o}\right)} - 3 \frac{\ln\left(1+\frac{\alpha\lambda}{a_o}\right)}{\left(1+\frac{\alpha\lambda}{a_o}\right)} - 3 \ln\left(1+\frac{\alpha\lambda}{a_o}\right) + \frac{\alpha\lambda/a_o}{\left(1+\frac{\alpha\lambda}{a_o}\right)} \right] \qquad \{3\text{-}103\}$$

3.4.3 Network Function H'(s) of the Complete Equivalent

For the complete equivalent, by previous definition:

$$H'(s) = \frac{1}{A'(s)}$$

where:

$$A'(s) = A_1 + sC_iB_1 \qquad \{3\text{-}104\}$$

and:

$$A_1 = 1 + a_1s + a_2s^2 + a_3s^3 + \cdots\cdots\cdots \qquad \{3\text{-}105\}$$

$$B_1 = b_o + b_1s + b_2s^2 + \cdots\cdots\cdots\cdots\cdots \qquad \{3\text{-}106\}$$

Substituting {3-105} and {3-106} into {3-104} yields:

$$A'(s) = 1 + (a_1+C_ib_o)s + (a_2+C_ib_1)s^2 + (a_3+C_ib_2)s^3 + \cdots\cdots$$

which can be expressed as:

$$A'(s) = 1 + a'_1s + a'_2s^2 + a'_3s^3 + \cdots\cdots\cdots\cdots \qquad \{3\text{-}107\}$$

where the modified coefficients are defined as follows:

$$\begin{aligned} a'_1 &= a_1 + C_ib_o \\ a'_2 &= a_2 + C_ib_1 \\ a'_3 &= a_3 + C_ib_2 \end{aligned} \qquad \{3\text{-}108\}$$

In general form, {3-107} and {3-108} may be expressed as:

$$A'(s) = 1 + \sum_{n=1}^{\infty} a'_ns^n \qquad \{3\text{-}109\}$$

where:

$$a'_n = a_n + C_ib_{n-1} \qquad \{3\text{-}110\}$$

and:

$$H'(s) = \frac{1}{1 + \sum_{n=1}^{\infty} a'_n s^n} \qquad \{3\text{-}111\}$$

The expressions for coefficients a_n and b_n can be expressed in more compact form by using the following substitutions:

$$\zeta = \frac{\rho c_o}{\pi \alpha^2}$$

$$\eta = 1 + \frac{\alpha \lambda}{a_o} \qquad \{3\text{-}112\}$$

$$\delta = \frac{\alpha}{c_o a_o}$$

Using the above substitutions yields:

$$a_1 = \zeta(\eta - 1 - \ln\eta) \qquad \{3\text{-}113\}$$

$$a_2 = \zeta^2 \left[\tfrac{1}{2}\ln^2\eta + (\eta+2)\ln\eta - 3(\eta-1)\right] \qquad \{3\text{-}114\}$$

$$a_3 = \zeta^3 \left[-\tfrac{1}{6}\ln^3\eta + \tfrac{1}{2}(\eta-3)\ln^2\eta - 4(\eta+\tfrac{3}{2})\ln\eta + 9(\eta-1)\right] \qquad \{3\text{-}115\}$$

and:

$$b_o = \delta\zeta\frac{\eta-1}{\eta} \qquad \{3\text{-}116\}$$

$$b_1 = \delta\zeta^2\left(\frac{\eta+1}{\eta}\ln\eta - 2\frac{\eta-1}{\eta}\right) \qquad \{3\text{-}117\}$$

$$b_2 = \delta\zeta^3\left(\tfrac{1}{2}\frac{\eta-1}{\eta}\ln^2\eta - 3\frac{\eta+1}{\eta}\ln\eta + 6\frac{\eta-1}{\eta}\right) \qquad \{3\text{-}118\}$$

3.5 Network Function of the Complete System

In accordance with the proposed scheme of waveform restoration (Figure I-6), the complete system is defined as follows:

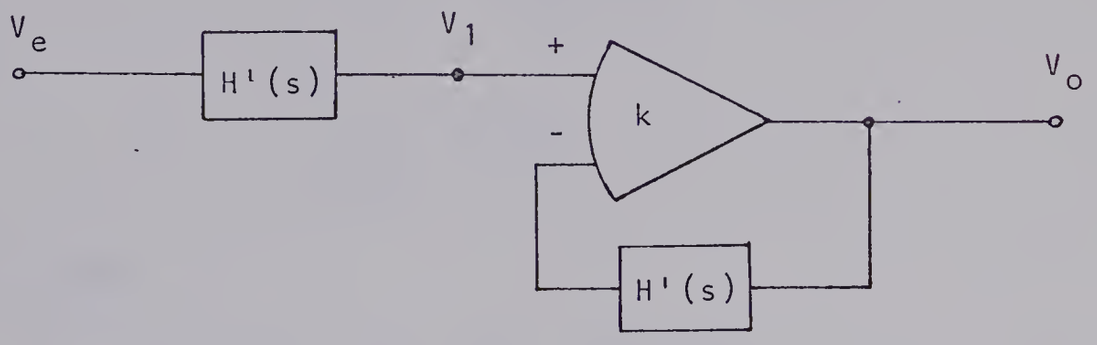

Figure III-5
The Complete System

The network function for the complete system is defined as:

$$H''(s) = \frac{V_o}{V_e} \qquad \{3\text{-}119\}$$

where: V_o = restored waveform

V_e = signal applied to electrode

k = open-loop gain of amplifier

With perfect restoration H''(s) = 1 for all frequencies.

Note: The operational amplifier is assumed to be ideal with infinite input impedance, zero output impedance, and open-loop gain k. (see Appendix VI)

The development to follow will establish the frequency dependance of H''(s) and is based on a knowledge of the network function of the complete equivalent H'(s).

From Figure III-5 we have:

$$V_o = k\,[V_1 - H'(s)V_o] = kV_1 - kH'(s)V_o$$

This yields:

$$\frac{V_o}{V_1} = \frac{k}{1 + kH'(s)}$$

Also:

$$\frac{V_1}{V_e} = H'(s)$$

From {3-119}:

$$H''(s) = \frac{V_o}{V_e} = \frac{V_o}{V_1} \cdot \frac{V_1}{V_e} = \frac{kH'(s)}{1 + kH'(s)} \qquad \{3\text{-}120\}$$

From {3-111}:

$$H'(s) = \frac{1}{1 + a'_1 s + a'_2 s^2 + a'_3 s^3 + \cdots\cdots\cdots} \qquad \{3\text{-}121\}$$

Combining {3-120} and {3-121} yields:

$$H''(s) = \frac{k}{k+1} \cdot \frac{1}{1 + c_1 s + c_2 s^2 + c_3 s^3 + \cdots\cdots} \qquad \{3\text{-}122\}$$

where:

$$c_1 = \frac{a'_1}{k+1}$$

$$c_2 = \frac{a'_2}{k+1} \qquad \{3\text{-}123\}$$

$$c_3 = \frac{a'_3}{k+1}$$

3.6 Network Function for Woodbury's Equalization

As previously stated in Chapter I, Woodbury[4] used restoration by equalization based on the simple two-element model of the electrode. To facilitate a comparison of the proposed equalization scheme and Woodbury's first-order technique, the transfer function is developed for the complete system where the network in the feedback loop of the amplifier is the simple two-element model. This system is presented in Figure III-6.

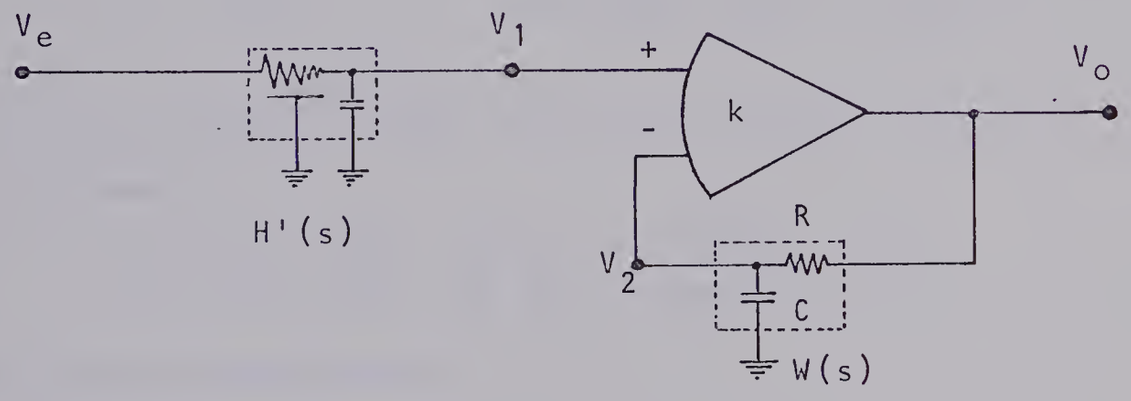

Figure III-6
Woodbury's Equalization System

where: $H'(s)$ = transfer function for proposed model

R = total electrode resistance

$$= \int_0^{\lambda} r(x)\,dx$$

C = total shunting capacitance

$$= \int_0^{\lambda} c(x)\,dx + C_i$$

$W(s)$ = transfer function of Woodbury's model

The network function for Woodbury's two-element model is defined as:

$$W(s) = \frac{V_2}{V_o} = \frac{1}{1+sT} \quad ; \quad T=RC \qquad \{3\text{-}124\}$$

For the feedback amplifier:

$$\frac{V_o}{V_1} = \frac{k}{1+kW(s)} = \frac{k(1+sT)}{(1+k)+sT} \qquad \{3\text{-}125\}$$

From {3-111} we have:

$$\frac{V_1}{V_e} = H'(s) = \frac{1}{1 + a'_1 s + a'_2 s^2 + a'_3 s^3 + \cdots} \qquad \{3\text{-}126\}$$

Using {3-125} and {3-126} the overall system transfer function becomes:

$$H'''(s) = \frac{V_o}{V_e} = \frac{V_o}{V_1} \cdot \cdot \frac{V_1}{V_e} = \frac{k(1+sT)}{(1+k)+sT} H'(s)$$

This may be expressed as:

$$H'''(s) = \frac{k}{1+k} \frac{1 + sT}{1 + d_1 s + d_2 s^2 + d_3 s^3 + d_4 s^4 + \cdots\cdots}$$

where:

$$d_1 = a'_1 + \frac{T}{1+k}$$

$$d_2 = a'_2 + \frac{a'_1 T}{1+k} \qquad \{3\text{-}127\}$$

$$d_3 = a'_3 + \frac{a'_2 T}{1+k}$$

$$d_4 = \frac{a'_3 T}{1+k}$$

CHAPTER IV

NUMERICAL ANALYSIS

4.1 Introduction

In the preceding pages of Chapter III the accepted equivalent circuit for the microelectrode probe in its measuring environment was analysed mathematically in terms of general physical constants.

The primary objective in this chapter is to assume reasonable numerical values for the describing constants and use these values in a qualitative evaluation of the complete system's stability. The relationships presented in section 3.5 will form the basis for this stability analysis.

The sections to follow present the assumed values for the describing physical constants which are used to determine numerical values for the coefficients characterizing the complete system's transfer function. The numerical analysis is conducted for both the proposed equalization scheme as well as for Woodbury's first-order system. A computer program used for Bode plot calculations is presented. With the use of the Digital Equipment PDP8/S computer, Bode plots for a number of test cases are calculated. These results are used to extract information regarding the frequency and time domain characteristics of the complete system proposed for the equalization of the microelectrode.

4.2 Evaluation of Coefficients

4.2.1 Numerical Values of Constants

Prior to the evaluation numerically of the network function coefficients assumed values are required for the fundamental constants α, λ, c_o, a_o and ρ.

taper α

A value of 1/60 is assumed in accordance with Ling and Gerard.[3] This is the largest tolerable value for satisfactory results.

line length λ

A value of 0.2 cm is assumed in accordance with Woodbury.[4]

tip radius a_o

A value of 1.67×10^{-5} cm is assumed based on a tip diameter of 0.5 microns and a lumen 2/3 of the outer diameter.

capacitance distribution c_o

A value of 10 pf/cm is assumed based on the results of Appendix VII and in accordance with Nastuk and Hodgkin.[2]

electrolyte resistivity ρ

A value of 4 ohm-cm is assumed based on the results of Appendix VIII.

4.2.2 Coefficients for the Distributed R-C Line

With the following values assumed for the fundamental constants:

$$\rho = 4 \text{ ohm-cm}$$

$$a_o = 1.67 \times 10^{-5} \text{ cm}$$

$$c_o = 10 \text{ pf/cm}$$

$$\alpha = 1/60$$

$$\lambda = 0.2 \text{ cm}$$

substitution in to {3-112} yields:

$$\zeta = 4.58 \times 10^{-8} \text{ sec}$$

$$\eta = 201$$

$$\delta = 10^{14} \text{ fd}^{-1}$$

and further substitution into {3-113} → {3-118} yields:

$$a_1 = 8.9 \times 10^{-6} \text{ sec}$$

$$a_2 = 0.98 \times 10^{-12} \text{ sec}^2$$

$$a_3 = 0.026 \times 10^{-18} \text{ sec}^3$$

$$b_o = 4.5 \times 10^{6} \text{ ohm}$$

$$b_1 = 0.69 \text{ ohm}^2\text{-fd}$$

$$b_2 = 3.8 \times 10^{-8} \text{ ohm}^3\text{-fd}^2$$

4.2.3 Coefficients for the Complete Equivalent

Using the numerical values established in section 4.2.2 and the relationships of {3-108} yields the

a'_n coefficients for the complete equivalent, expressed for a number of C_i values. Numerical values for these coefficients are presented in Table IV-1.

Table IV-1

	C_i (pf)			
COEFFICIENT	2	5	10	20
a'_1 ($\times 10^{-6}$ sec)	18	31	53.9	98.9
a'_2 ($\times 10^{-12}$ sec^2)	2.4	4.4	7.88	14.78
a'_3 ($\times 10^{-18}$ sec^3)	0.1	0.22	0.406	0.786

4.2.4 Coefficients for the Complete System

Using the numerical values established in section 4.2.3 and the relationships of {3-123} yields the c_n coefficients for the complete system. Numerical values for these coefficients are presented in Table IV-2.

4.2.5 Coefficients for Woodbury's System

In section 3.6 it was established that Woodbury's model is characterized by:

$$R = \int_0^{\lambda} r(x)\,dx$$

$$C = \int_0^{\lambda} c(x)\,dx + C_i$$

Using the numerical values assumed in section 4.2.1 we have:

Table IV-2

COEFFICIENT	k=100 C_i (pf)			k=200 C_i (pf)			k=500 C_i (pf)		
	2	5	20	2	5	20	2	5	20
c_1 ($\times 10^{-7}$ sec)	1.78	3.07	9.79	.895	1.54	4.92	.360	.619	1.975
c_2 ($\times 10^{-14}$ sec^2)	2.38	4.36	14.62	1.193	2.19	7.35	.479	.877	2.95
c_3 ($\times 10^{-21}$ sec^3)	0.99	2.18	7.79	.497	1.09	3.91	.200	.439	1.57

Table IV-3

COEFFICIENT	k=100 C_i (pf)			k=200 C_i (pf)			k=500 C_i (pf)		
	2	5	20	2	5	20	2	5	20
d_1 ($\times 10^{-6}$ sec)	18.2	31.3	99.9	18.1	31.2	99.4	18.0	31.1	99.1
d_2 ($\times 10^{-12}$ sec^2)	5.65	14.2	113.	4.03	9.32	64.1	3.06	6.38	34.6
d_3 ($\times 10^{-18}$ sec^3)	.533	1.61	15.5	.318	.919	8.16	.187	.500	3.74
d_4 ($\times 10^{-24}$ sec^4)	.018	.070	.781	.009	.035	.392	.004	.014	.157

$R = 4.56$ Mohms

$C = 2\ pf + C_i$

with: $T = RC$

we have: $T = 18.24\ \mu sec$ for $C_i = 2\ pf$

$T = 31.92\ \mu sec$ for $C_i = 5\ pf$

$T = 100.32\ \mu sec$ for $C_i = 20\ pf$

Using these values, the numerical values established in section 4.2.3 and the relationships of {3-127} yields the d_n coefficients for Woodbury's system. Numerical values for these coefficients are presented in Table IV-3.

4.3 Test for Stability

With numerical values established for the coefficients of the complete equivalent, Routh's stability criterion (Appendix IX) can be applied to the characteristic equation of the feedback system:

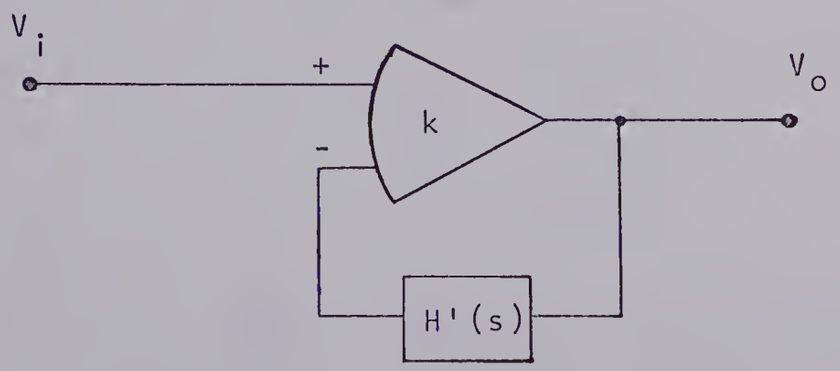

$$a'_3 s^3 + a'_2 s^2 + a'_1 s + (k+1) = 0$$

Numerical evaluation of the Routhian arrays for the four test cases yields the following information regarding system stability:

C_i (pf)	allowable k for stability
2	$-1<k<431$
5	$-1<k<619$
10	$-1<k<1045$
20	$-1<k<1859$

These results indicate that the feedback system is conditionally stable and that increasing values of C_i guarantee stability for wider ranges of amplifier open-loop gain k.

An examination of the characteristic equation for Woodbury's equalization system shows that this system is unconditionally stable for all positive k.

4.4 Program for Bode Plot Calculations

4.4.1 Development

For the general case, the transfer function takes the following form:

$$G(s) = \frac{U(s)}{V(s)} = \frac{\sum_{n=0}^{\infty} u_n s^n}{\sum_{m=0}^{\infty} v_m s^m}$$

or:

$$G(s) = \frac{u_o + u_1 s + u_2 s^2 + \cdots\cdots\cdots\cdots}{v_o + v_1 s + v_2 s^2 + \cdots\cdots\cdots\cdots}$$

In the sinusoidal steady-state $s=j\omega$, and therefore:

$$G(j\omega) = \frac{(u_o - u_2\omega^2 + \cdots\cdots\cdots) + j(u_1\omega - u_3\omega^3 + \cdots\cdots\cdots)}{(v_o - v_2\omega^2 + \cdots\cdots\cdots) + j(v_1\omega - v_3\omega^3 + \cdots\cdots\cdots)}$$

$$= |G(j\omega)| \angle \phi(\omega)$$

where:

$$|G(j\omega)| = \frac{(u_o - u_2\omega^2 + \cdots\cdots)^2 + (u_1\omega - u_3\omega^3 + \cdots)^2}{(v_o - v_2\omega^2 + \cdots\cdots)^2 + (v_1\omega - v_3\omega^3 + \cdots)^2}$$

and:

$$\phi(\omega) = \arctan \frac{u_1\omega - u_3\omega^3 + \cdots}{u_o - u_2\omega^2 + \cdots\cdot} - \arctan \frac{v_1\omega - v_3\omega^3 + \cdots\cdot}{v_o - v_2\omega^2 + \cdots\cdot}$$

For the transfer function of interest:

$$n = 0$$
$$m = 3.$$

4.4.2 Computer Program

The computer program to follow was written for the case where:

$$n = 6$$
$$m = 7.$$

Provisions are made for the arbitrary selection of the desired frequency range and the desired sampling density of log-magnitude calculations. The output lists frequency, absolute magnitude, magnitude in decibels and phase angle. The language is FORTRAN IV and the machine used is the Digital Equipment PDP8/S.

```
C; BODE PLOTTER
   DIMENSION A(6), B(7)
Ø; FORMAT(/,"NUMERATOR COEFFICIENTS ARE:",/)
```

```
    TYPE Ø
    I=1
 1; FORMAT(E)
 2; ACCEPT 1, A(I)
    I=I+1
    IF(I-7) 2,3,3
 3; CONTINUE
 4; FORMAT(/,"DENOMINATOR COEFFICIENTS ARE:",/)
    TYPE 4
    I=1
 5; ACCEPT 1,B(I)
    I=I+1
    IF(I-8) 5,6,6
 6; CONTINUE
 7; FORMAT(/,"FREQUENCY(LOWER,FREQUENCY(HIGHER,
    DELTA",/)
    TYPE 7
 8; FORMAT(/,E,E,E,/)
    ACCEPT 8,F1,F2,DF
    F=F1
1Ø; W=F*2.000*3.14159
    RA=A(2)*(W**4)-A(4)*(W**2)+A(6)
    AI=A(1)*(W**5)-A(3)*(W**3)+A(5)*W
    RB=-B(1)*(W**6)+B(3)*(W**4)-B(5)*(W**2)+B(7)
    BI=B(2)*(W**%)-B(4)*(W**3)+B(6)*W
    ABA=SQTF(RA*RA+AI*AI)
    ABB=SQTF(RB*RB+BI*BI)
    ANGA=ATNF(AI/RA)
    ANGA=ANGA*57.295779
    IF(RA) 11,12,12
11; ANGA=ANGA+18Ø.Ø
12; CONTINUE
    ANGB=ANGB*57.295779
    ANGB=ATNF(BI/RB)
    IF(RB) 13,14,14
13; ANGB=ANGB+18Ø.Ø
14; CONTINUE
    GSV=ABA/ABB
    ANGS=ANGA-ANGB
    DBS=2Ø.Ø*LOGF(GSV)/2.3Ø3
    TYPE 16,F,GSV,DBS,ANGS
16; FORMAT(/,E,E,E,E)
    IF(F-F2) 17,17,18
17; CONTINUE
    F=(1Ø.Ø**(1.Ø/DF))*F
    GO TO 1Ø
18; CONTINUE
    GO TO Ø
    END
```

4.5 Results of Bode Plot Calculations

With the use of the coefficients of sections 4.2.3, 4.2.4 and 4.2.5, the computer program of section 4.4.2, and the Digital Equipment PDP8/S machine, Bode log-magnitude-phase calculations were made for a variety of test cases. These results are presented graphically in Figures IV-1 to IV-3 in the form of magnitude frequency response curves (fixed C_i; variable k) for the network functions outlined in Table IV-4.

Table IV-4

H'(s)	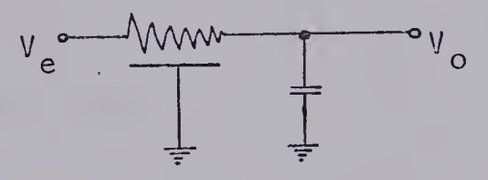	microelectrode complete equivalent
H''(s)	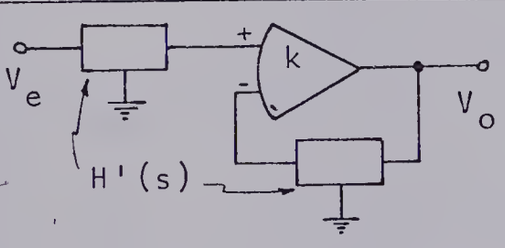	proposed equalization system
H'''(s)	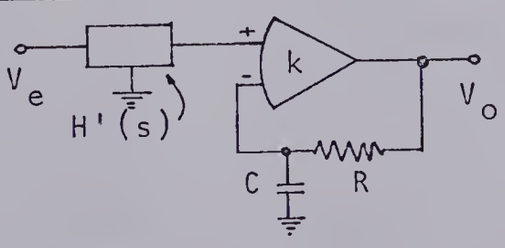	Woodbury's equalization system

Tables IV-5 and IV-6 list the 3db (down) cutoff frequencies and approximate risetimes for each of the selected test cases.

Table IV-5

Unequalized Microelectrode: H'(s)

C_i	f_{3db} (Hz)	t_r* (μsec)
2	8.7k	40
5	5k	70
20	1.5k	230

*see Appendix X

Table IV-6

Equalized Microelectrode

C_i (pf)	open-loop gain k	PROPOSED H''(s)		WOODBURY'S H'''(s)	
		f_{3db} (Hz)	t_r* μsec	f_{3db} (Hz)	t_r* μsec
2	100	1.5M	.23	780k	.45
5	100	900k	.39	500k	.70
20	100	160k	2.2	160k	2.2
2	200	2.2M	.16	1.17M	.30
5	200	1.7M	.21	900k	.39
20	200	450k	.78	340k	1.03
2	500	3.1M	.11	1.5M	.23
5	500	2.5M	.14	1.3M	.27
20	500	1.4M	.25	700k	.50

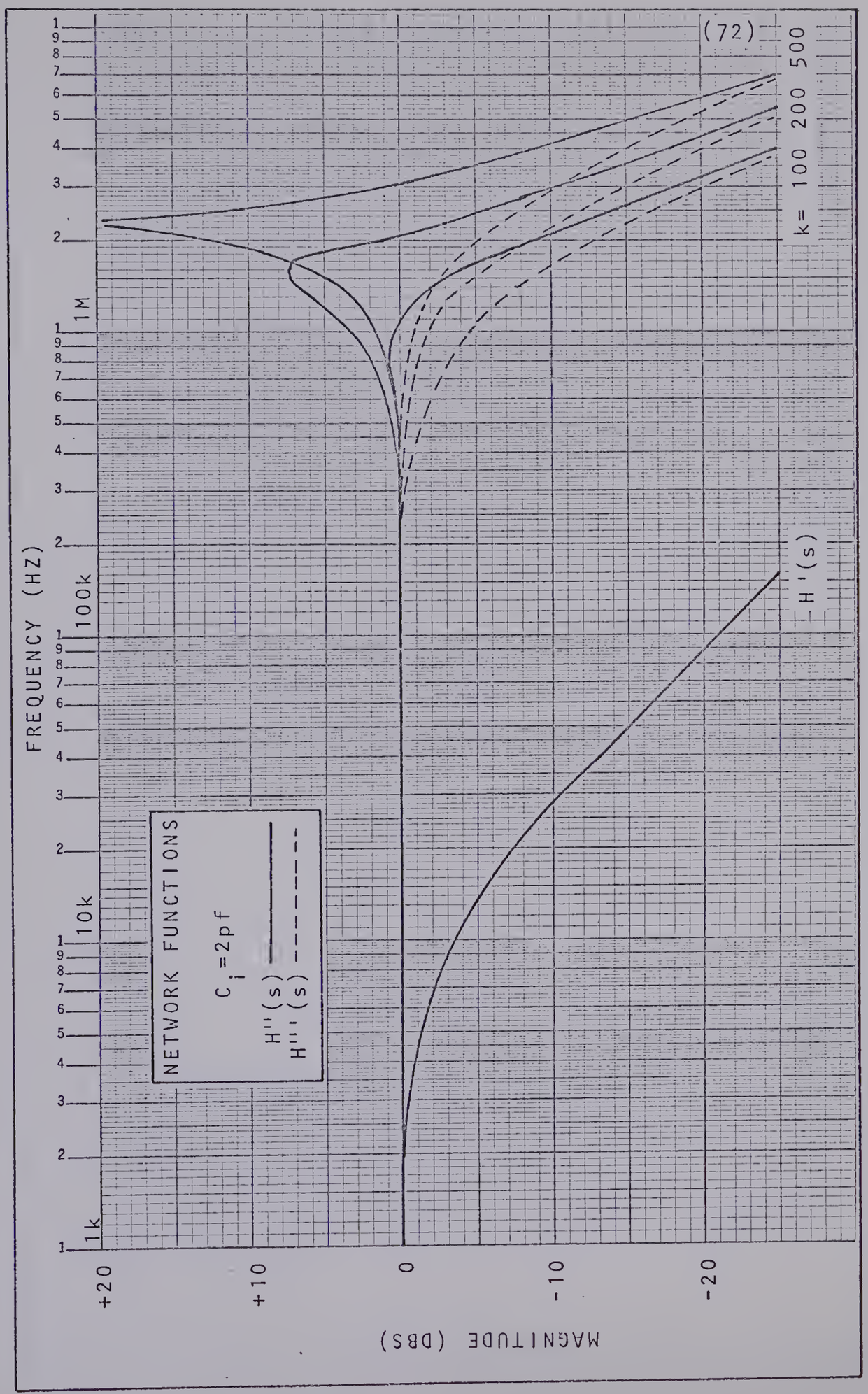
(72)
k= 100 200 500
H'(s)
NETWORK FUNCTIONS
C_i=2pf
H''(s)
H'''(s)
FREQUENCY (HZ)
1k
10k
100k
1M
+20
+10
0
-10
-20
MAGNITUDE (DBS)

Figure IV-1

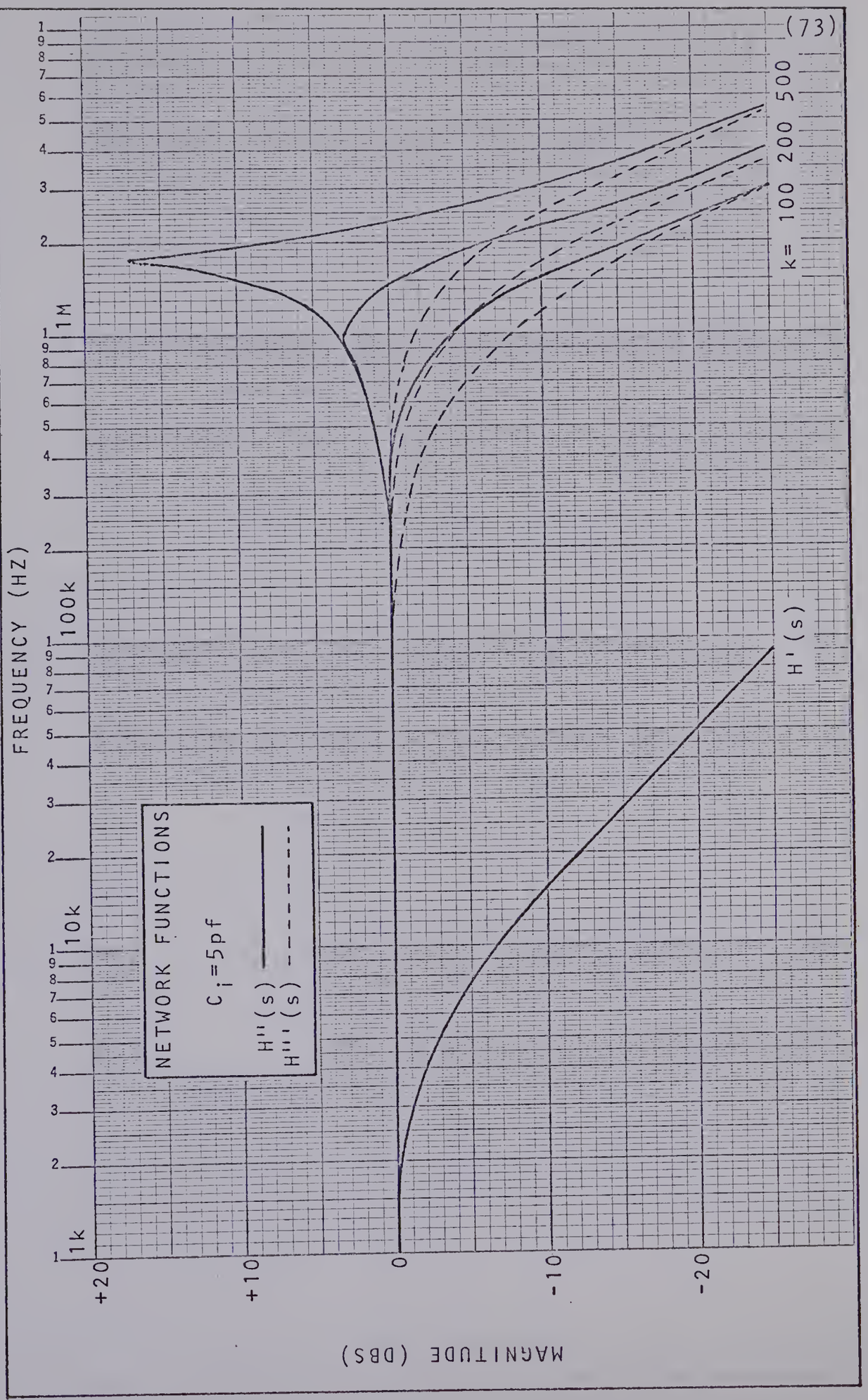
MAGNITUDE (DBS)
+20
+10
0
-10
-20
FREQUENCY (HZ)
1k
10k
100k
1M
NETWORK FUNCTIONS
C_i=5pf
H''(s)
H'''(s)
H'(s)
k= 100 200 500

Figure IV-2

Figure IV-3

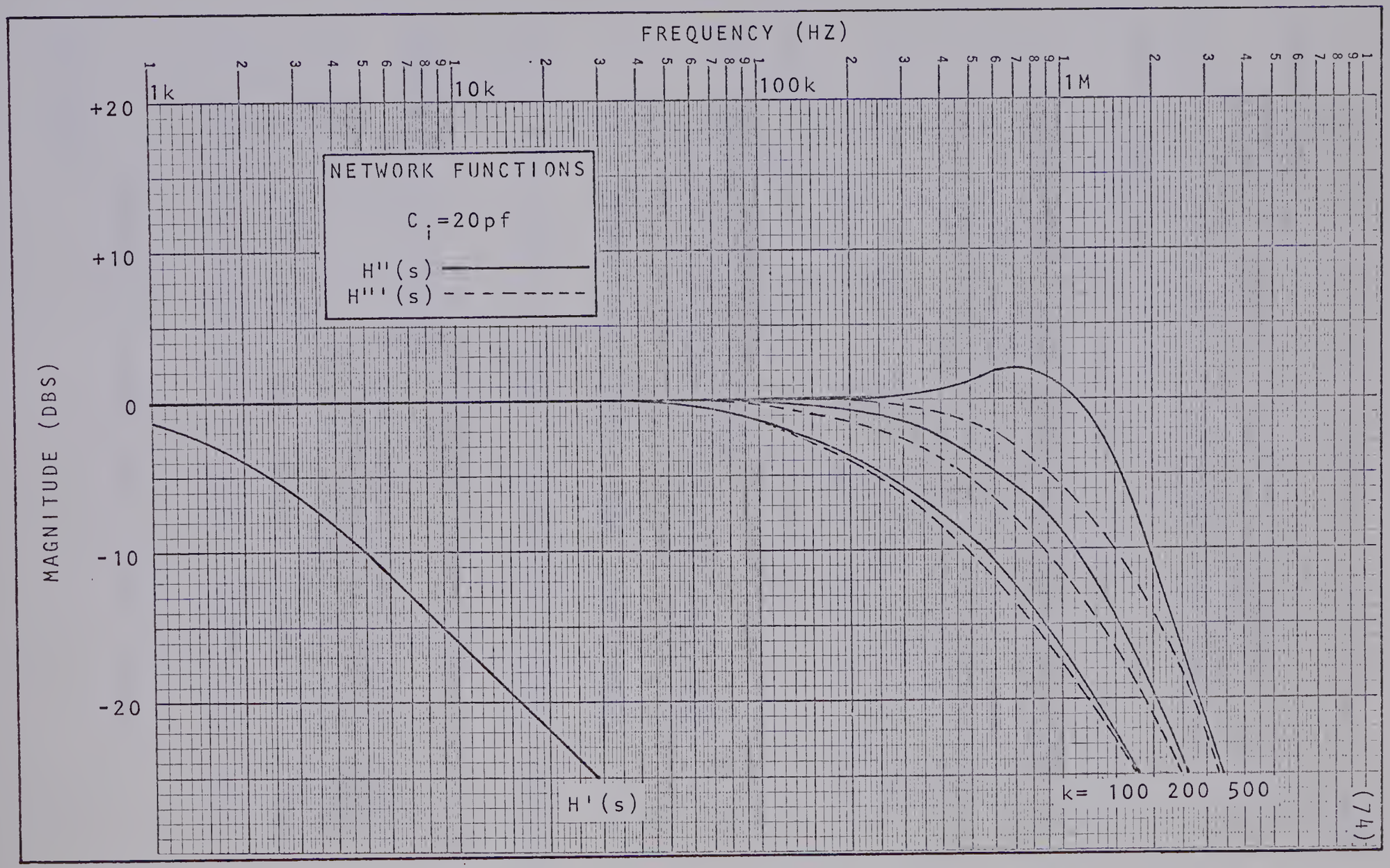
FREQUENCY (HZ)
1k
10k
100k
1M
+20
+10
0
-10
-20
MAGNITUDE (DBS)
NETWORK FUNCTIONS
C_i=20pf
H''(s)
H'''(s)
H'(s)
k= 100 200 500
(74)

4.6 Conclusions

Based on the numerical results established in this chapter the following may be concluded with respect to:

system stability (section 4.3)

For the proposed equalization scheme the system is conditionally stable with lower and upper limits existing for the amplifier open-loop gain parameter k (with C_i fixed). It has been established that higher values of C_i guarantee higher allowable values of k.

For Woodbury's equalization scheme the system is unconditionally stable for all positive k.

low frequency ($f \ll f_{3db}$) error

Since, from equations {3-122} and {3-127}:

$$|H''(s)| = |H'''(s)| = \frac{k}{1+k} \quad \text{for } f \ll f_{3db}$$

values of k should be high to guarantee minimum magnitude errors.

bandwidth and risetime

On the basis of Bode calculations (Table IV-6), for both equalization systems, increasing system bandwidth and hence decreasing system risetime are realized with decreasing values of C_i and/or increasing values of k.

A comparative examination of both systems indicates:

1. A very significant improvement in risetime relative to the unequalized microelectrode.
2. A definite improvement in risetime for the proposed scheme relative to Woodbury's scheme (at fixed k). Maximum improvement is realized at low C_i values.

i.e. for k=100 and C_i= 2pf: 92% extension in BW

C_i= 5pf: 80% extension in BW

C_i=20pf: 0% extension in BW

Note: The numerical analysis in this chapter has been based on assumed values for the governing physical constants which yield a total electrode resistance in the order of 5 megohms. Interpretation of the numerical results should be made with this factor in mind. The conclusions are based only on the relative comparison of the network transfer functions analysed and the inherent trends established.

CHAPTER V

CONCLUSIONS AND SUGGESTIONS FOR FURTHER RESEARCH

5.1 Conclusions

The author feels there are two main contributions made by this investigation. Firstly, the analysis of the distributed R-C line for the special case encountered and, secondly, the equalization proposal for glass microelectrodes used in intracellular action potential measurements.

As was mentioned previously, analysis of distributed parameter networks has received the attention of many investigators in recent years. The solution, in closed form, of the general partial differential equations describing an arbitrary {r(x) and c(x) functions} non-uniform R-C line has not been found. Detailed analysis has been isolated to a number of special cases. The author feels that this investigation provides information of interest to these researchers in that the special case peculiar to this thesis is unique. Of particular significance is: the sinusoidal steady-state solutions for line voltage and current (pages 31-32); the general solution via Legendre's transformation (page 31); the network z-parameters as a basis for establishing any two-port parameter set (page40); and the derivation of the network forward transfer function H(s) for the open circuit termina-

tion case (page 43) and H'(s) for the capacitive termination case (page 50).

In this investigation a proposal utilizing waveform restoration by equalization has been made to correct inherent distortion contributed by the low-pass nature of the glass microelectrode used in the measurement of cellular action potentials. Analysis has yielded: a proposed equivalent circuit; a detailed mathematical description of the microelectrode based on the assumed electrical equivalent; a transfer function description of the proposed equalization scheme; and a numerical evaluation of a number of test cases. On the basis of this analysis the author concludes that the proposed restoration scheme is indeed feasible; however, depending on measurement requirements, the degree of improvement to be gained over Woodbury's scheme may not justify further investigation. Woodbury's scheme has the definite advantage of being unconditionally stable (within the constraints of the assumptions made) for all positive k; with increasing k being consistent with increasing bandwidth and decreasing low frequency error. The advantage associated with the proposed scheme is increased system bandwidth (for low C_i) due to more exact equalization and the possibility of utilizing the positive boost which occurs as the system approaches instability.

5.2 Suggestions for Further Research

It is considered beyond the realm of this investigation to make specific quantitative design proposals which would result in an immediate physical realization of the restoration circuitry. However, on the basis of the investigation as it stands, and assuming that sufficient motivation exists for improvements to the degree implied by the results of this study, further research could be directed in the following areas:

1. A numerical analysis for a wide range of realizable electrodes in terms of assumed physical constants to determine whether the success of the proposed scheme is electrode dependent.
2. An investigation of the noise characteristics of the proposed equalization scheme.
3. A study of the effect of non-ideal operational amplifier characteristics on the response of the proposed equalization system.
4. A study of the possibility of economic fabrication of the required distributed parameter network with provision for external control of effective line length.

REFERENCES

(1) E. Amatniek, "Measurement of Bioelectric Potentials with Microelectrodes and Neutralized Input Capacity Amplifiers", *IRE Transactions on Medical Electronics*, PG ME10, pp.3-14; March, 1958.

(2) W.L. Nastuk and L.A. Hodgkin, "The Electrical Activity of Single Muscle Fibers", *J. Cell. Comp. Physiol.*, vol. 35, pp. 39-72; February, 1950.

(3) G. Ling and R.W. Gerard, "The Normal Membrane Potential of Frog Sartorius Fibers", *J. Cell. Comp. Physiol.*, vol. 34, pp. 383-396; December, 1949.

(4) J.W. Woodbury, "Direct Membrane Resting and Action Potentials from Single Myelinated Nerve Fibers", *J. Cell. Comp. Physiol.*, vol. 39, pp.323-339; April, 1952.

(5) B. Frankenhaeuser, B.D. Lindley and R.S. Smith, "Potentiometric Measurement of Membrane Action Potentials in Frog Muscle Fibers", *J. Physiol.* (1966), 183, pp.152-166.

(6) J.T. Alexander and W.L. Nastuk, "An Instrument for the Production of Microelectrodes Used in Electrophysiological Studies", *Rev. Sci. Instr.*, vol. 24, p. 528; July, 1953.

(7) D.B. Cater and I.A. Silver, "Microelectrodes and Electrodes Used in Biology", *Reference Electrodes, Theory and Practice*, Chapter Eleven; Ives and Janz, Academic Press, 1961.

(8) R.C. Gesteland, B. Howland, J.V. Lettvin and W.H. Pitts, "Comments on Microelectrodes", *Proceedings of the IRE*, pp.1856-1862; November, 1959.

(9) D.W. Kennard, "Glass Microcapillary Electrodes Used for Measuring Potential in Living Tissue", *Electronic Apparatus for Biological Research*, (P.E.K. Donaldson, ed.) pp.534-567; Butterworths, London, 1958.

(10) J.W. Moore and J.H. Gebhart, "Stabilized Wide-Band Potentiometric Preamplifiers", *Proceedings of the IRE*, pp. 1928-1930; September, 1962.

(11) H. Fein, "Solid-State Electrometers with Input-Capacitance Neutralization", *IEEE Transactions on Bio-Medical Engineering*, pp.13-18; January-April, 1964.

(12) C. Guld, "Cathode Follower and Negative Capacitance as High Input Impedance Circuits", *Proceedings of the IRE*, pp.1912-1927; September, 1962.

(13) R.L. Tucker, "The Design of a Field Effect Transistor Amplifier for Measuring Bio-Electrical Action Potentials", *M.Sc. Thesis, University of Alberta;* April, 1965.

(14) W.C. Elmore, "The Transient Response of Damped Linear Networks with Particular Regard to Wideband Amplifiers", *J. Appl. Phys.*, vol. 19, pp.55-63; January, 1948.

(15) C.K. Hager, "Network Design of Microcircuits", *Electronics*, vol. 32, pp.44-49; September, 1959.

(16) W.W. Happ and P.S. Castro, "Distributed Parameter Circuit Design Techniques", *Proceedings of the National Electronics Conference*, vol. 17, pp.45-68; 1961.

(17) W.W. Happ and W.D. Fuller, "Design Procedures for Film Type Distributed Parameter Circuits", *Proceedings of NEC*, vol. 17, pp.597-610; 1961.

(18) M.J. Hellstrom, "Symmetrical RC Distributed Networks", Correspondence, *Proceedings of the IRE*, pp.97-98; January, 1962.

(19) W.W. Happ, "Synthesis of Distributed Parameter RC Networks", Correspondence, *Proceedings of the IRE*, pp.483-484; April, 1962.

(20) M.J. Hellstrom, "A New Class of Distributed RC Ladder Networks", Correspondence, *Proceedings of the IRE*, pp. 1989-1990; September, 1962.

(21) M.J. Hellstrom, "Equivalent Distributed RC Networks or Transmission Lines", *IRE Transactions on Circuit Theory*, vol. CT-9, pp.247-251; September, 1962.

(22) K.W. Heizer, "Distributed RC Networks with Rational Transfer Functions", *IRE Transactions on Circuit Theory*, vol. CT-9, pp.356-362; December, 1962.

(23) W.M. Kaufman and S.J. Garrett, "Tapered Distributed Filters", *IRE Transactions on Circuit Theory*, vol. CT-9, pp.329-336; December, 1962.

(24) M.S. Ghausi and G.J. Herskowitz, "The Transient Response of Tapered Distributed RC Networks", *IRE Transactions on Circuit Theory*, Correspondence, vol. CT-10, pp.443-445; September, 1963.

(25) R.A. Dell and S.L. Hakimi, "Limitations of Distributed RC Filters", *Proceedings of NEC*, vol. 20, 1964.

(26) S.C. Dutta Roy, "Matrix Parameters of Nonuniform Transmission Lines", Correspondence, *IEEE Transactions on Circuit Theory*, vol. CT-12, pp.142-143; March, 1965.

(27) S.C. Dutta Roy, "Some Exactly Solvable Nonuniform RC Lines", Correspondence, *IEEE Transactions on Circuit Theory*, vol. CT-12, pp.141-142; March, 1965.

(28) L. Gruner, "The Steady-State Characteristics of Nonuniform RC Distributed Networks and Lossless Lines", *IEEE Transactions on Circuit Theory*, vol. CT-12, pp.241-247; June, 1965.

(29) A.G. Lindgren, "Transfer Characteristics of a Class of Distributed RC Networks", Correspondence, *Proceedings of the IEEE*, pp.625-626; June, 1965.

(30) E.N. Protonotarios and O. Wing, "Delay and Rise Time of Arbitrarily Tapered R-C Transmission Lines", *IEEE International Convention Record*, Part 7, pp.1-6; 1965.

(31) J.J. Kelly and M.S. Ghausi, "Tapered Distributed RC Networks with Similar Immittances", *IEEE Transactions on Circuit Theory*, vol. CT-12, pp.554-558; December, 1965.

(32) F. Ayres, Jr., "Linear Equations with Variable Coefficients", *Theory and Problems of Differential Equations*, Chapter 17; Schaum's Outline Series.

(33) L.P. Huelsman, "Circuit Theory of Matrices", *Circuits, Matrices and Linear Vector Spaces*, Chapter 3; McGraw-Hill, 1963.

(34) Gustav Doetsch, "Partial Differential Equations", *Guide to the Applications of Laplace Transforms*, Chapter 5; Van Nostrand, 1961.

(35) M. Javid and E. Brenner, "Transmission Lines I - Transients", *Analysis, Transmission and Filtering of Signals*, Chapter 11; McGraw-Hill, 1963.

(36) A.S. Jackson, "Partial Differential Equations", *Analog Computation*, Chapter 8; McGraw-Hill, 1960.

(37) A.S. Jackson, "The Basic Analog Computer", *Analog Computation*, Chapter 2; McGraw-Hill, 1960.

(38) P. Dransfield, "Engineering Systems and Automatic Control", *The Stability of Components and Systems*, Chapter 6; Prentice-Hall, 1968.

(39) J. Millman and C. Halkias, *Electronic Devices and Circuits*, Chapter 16, pp.465-466; McGraw-Hill, 1967.

APPENDIX I

DERIVATION OF FUNCTION r(x) FOR THE MICROELECTRODE

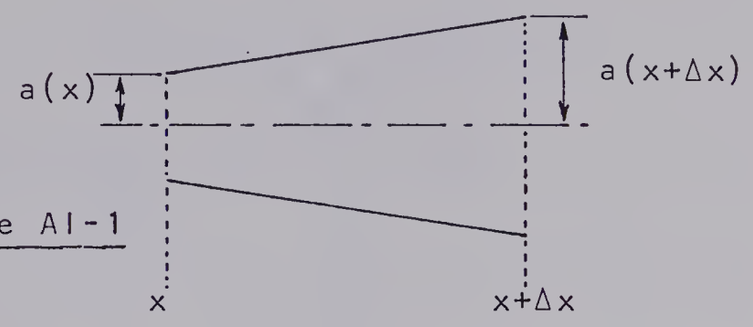

Figure AI-1

Figure AI-1 represents a differential element of the electrolytic column with a(x) representing the radius of the column at position x along the column. For this element:

$$a(x) = a_o+\alpha x$$

$$A(x) = \pi(a_o+\alpha x)^2$$

$$a(x+\Delta x) = a_o+\alpha(x+\Delta x)$$

$$A(x+\Delta x) = \pi\{a_o+\alpha(x+\Delta x)\}^2$$

Consider the resistance R of this element:

$$\Delta R = \rho \frac{\Delta x}{\text{average area}}$$

where: $$\text{average area} = \tfrac{1}{2}\{A(x)+A(x+\Delta x)\}$$

$$= A(x)+\tfrac{1}{2}\pi\alpha(2a_o\Delta x+2\alpha x\Delta x+\alpha\Delta x^2)$$

Therefore:

$$r(x) = \frac{dR}{dx} = \lim_{\Delta x\to 0}\frac{\Delta R}{\Delta x} = \frac{\rho}{A(x)} = \frac{\rho}{\pi(a_o+\alpha x)^2}$$

APPENDIX II

DERIVATION OF THE PARTIAL DIFFERENTIAL EQUATION WHICH CHARACTERIZES A GENERAL DISTRIBUTED R-C NETWORK[12]

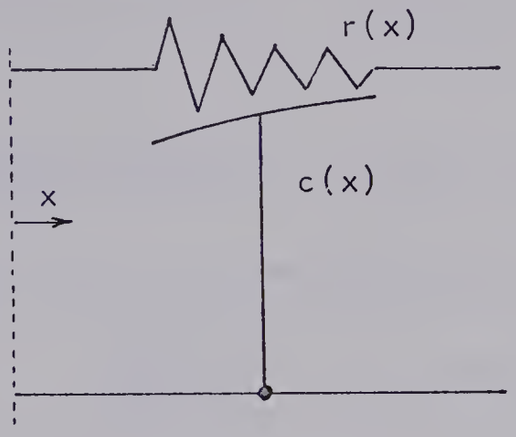

Figure AII-1
Symbolic Representation

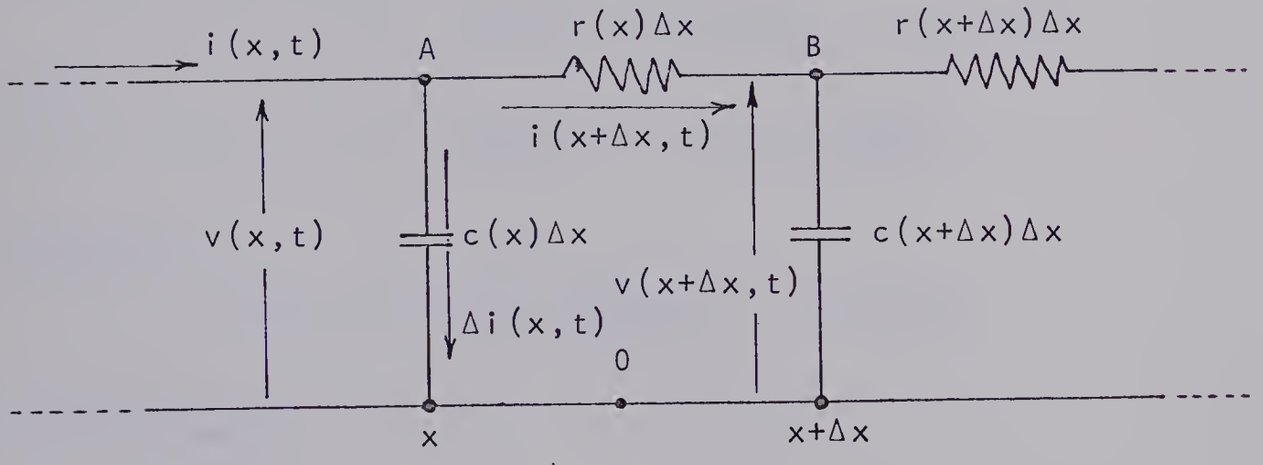

Figure AII-2
A Differential Element

The following development is general and applicable to any arbitrarily tapered R-C line. Attention is restricted to one dimensional current flow. The introduction of tapers results in resistance per unit length r(x) and capacitance per unit length c(x) where x is the space parameter in the direction of current flow. Figure AII-1 illustrates the

accepted symbolic representation of a tapered distributed R-C network. Figure AII-2 represents a differential element of this network.

Consider the loop equation of AB0:

$$v(x,t) - i(x+\Delta x,t)\,r(x)\Delta x - v(x+\Delta x,t) = 0$$

Therefore:

$$\frac{v(x+\Delta x,t) - v(x,t)}{\Delta x} = - i(x+\Delta x,t)\,r(x)$$

Consider the limit as $\Delta x \to 0$; the equation becomes:

$$\frac{\partial v(x,t)}{\partial x} = - i(x,t)\,r(x) \qquad \{1\}$$

Consider the node equation at A:

$$i(x,t) = \Delta i(x,t) + i(x+\Delta x,t)$$

Also:

$$\Delta i(x,t) = c(x)\Delta x \frac{\partial v(x,t)}{\partial t}$$

Therefore:

$$i(x,t) = c(x)\Delta x \frac{\partial v(x,t)}{\partial t} + i(x+\Delta x,t)$$

This becomes:

$$\frac{i(x+\Delta x,t) - i(x,t)}{\Delta x} = - c(x) \frac{\partial v(x,t)}{\partial t}$$

Consider the limit as $\Delta x \to 0$; the equation becomes:

$$\frac{\partial i(x,t)}{\partial x} = - c(x) \frac{\partial v(x,t)}{\partial t} \qquad \{2\}$$

With v and i functions of x and t, equations {1} and {2} can be written:

$$\frac{\partial v}{\partial x} = - r(x)\ i \quad \text{and} \quad \frac{\partial i}{\partial x} = - c(x)\ \frac{\partial v}{\partial t}$$

From {1}:

$$i = - \frac{1}{r(x)}\ \frac{\partial v}{\partial x}$$

Substituting into {2} yields:

$$\frac{\partial}{\partial x}\left[- \frac{1}{r(x)}\ \frac{\partial v}{\partial x}\right] = - c(x)\ \frac{\partial v}{\partial t}$$

Expanding the partial differentiation yields:

$$- \frac{1}{r(x)}\ \frac{\partial^2 v}{\partial x^2} + \frac{1}{\{r(x)\}^2}\ \frac{dr(x)}{dx}\ \frac{\partial v}{\partial x} = - c(x)\ \frac{\partial v}{\partial t}$$

Finally the equation becomes:

$$\frac{\partial^2 v}{\partial x^2} - \frac{1}{r(x)}\ \frac{dr(x)}{dx}\ \frac{\partial v}{\partial x} = r(x)c(x)\ \frac{\partial v}{\partial t} \qquad \{3\}$$

A similar development for current yields:

$$\frac{\partial^2 i}{\partial x^2} - \frac{1}{c(x)}\ \frac{dc(x)}{dx}\ \frac{\partial i}{\partial x} = r(x)c(x)\ \frac{\partial i}{\partial t} \qquad \{4\}$$

Both equations {3} and {4} govern the behavior of a distributed R-C line in which R and C are functions of x only.

APPENDIX III

TRANSFORMATION OF EQUATION {3-14}

Equation {3-14} has been expressed as:

$$(a_o+\alpha x)^2 \frac{d^2X}{dx^2} + 2\alpha(a_o+\alpha x) \frac{dX}{dx} + \frac{\rho c_o}{\pi} k^2 X = 0 \qquad \{1\}$$

This is an ordinary linear second-order differential equation with variable coefficients and is recognized as the second-order form of Legendre's Linear Equation.[32] The equation can be reduced to a linear equation with constant coefficients by means of the following transformation:

$$e^z = (a_o+\alpha x) \qquad \{2\}$$

The evolution of the transformation is as follows:

$$e^z \, dz = \alpha \, dx$$

$$\frac{dz}{dx} = \frac{\alpha}{a_o+\alpha x}$$

$$\frac{d^2z}{dx^2} = -\frac{\alpha^2}{(a_o+\alpha x)^2}$$

$$\frac{dX}{dx} = \frac{dX}{dz}\frac{dz}{dx} = \frac{\alpha}{a_o+\alpha x}\frac{dX}{dz}$$

Therefore:

$$(a_o+\alpha x) \frac{dX}{dx} = \alpha \frac{dX}{dz} \qquad \{3\}$$

Further:

$$\frac{d^2X}{dx^2} = \frac{d}{dx}\left[\frac{dX}{dz}\cdot\frac{dz}{dx}\right] = \frac{dz}{dx}\cdot\frac{d}{dx}\left[\frac{dX}{dz}\right] + \frac{d^2z}{dx^2}\frac{dX}{dz}$$

$$\frac{d}{dx} = \frac{\alpha}{a_o+\alpha x} \frac{d}{dz}$$

$$\frac{d^2X}{dx^2} = \frac{\alpha^2}{(a_o+\alpha x)^2} \left[\frac{d^2X}{dz^2} - \frac{dX}{dz} \right]$$

Therefore:

$$(a_o+\alpha x)^2 \frac{d^2X}{dx^2} = \alpha^2 \left[\frac{d^2X}{dz^2} - \frac{dX}{dz} \right] \qquad \{4\}$$

Substituting equations {3} and {4} into equation {1} yields the transformed equation {5} where:

$$X = X(z) \quad ; \quad X(x) \leftrightarrow X(z)$$

$$\frac{d^2X}{dz^2} + \frac{dX}{dz} + \frac{k^2 c_o \rho}{\pi \alpha^2} X = 0 \qquad \{5\}$$

APPENDIX IV

CONDITIONS ESTABLISHING det[A]=0

Consider the following:

$$[B] = [A]^{-1} = \frac{1}{\det[A]} \begin{bmatrix} a_{22} & -a_{12} \\ -a_{21} & a_{11} \end{bmatrix}$$

where: $\det[A] = a_{11}a_{22} - a_{12}a_{21}$

From previously developed expressions:

$$\det[A] = -\left(\frac{\pi\alpha}{2\rho}\right)^2 \{a_o(a_o+\alpha\lambda)\}^{\frac{1}{2}}(1-\theta'^2)\sinh\{\phi(0)-\phi(\lambda)\}$$

From the above expression:

1. $\det[A]=0$ for $(1-\theta'^2)=0$ or $\theta'^2=1$
2. $\det[A]=0$ for $\sinh\{\phi(0)-\phi(\lambda)\}=0$ or $\phi(0)-\phi(\lambda) = 0$

Expanding on these statements:

statement 1:

$$\theta' = \left[1 + j\omega\frac{4\rho c_o}{\pi\alpha^2}\right]^{\frac{1}{2}}$$

$$\theta'^2 = 1 \quad \text{for } j\omega\frac{4\rho c_o}{\pi\alpha^2} = 0 \quad \text{or } \omega = 0$$

statement 2:

$$\{\phi(0)-\phi(\lambda)\} = \tfrac{1}{2}\theta' \ln\left(\frac{a_o}{a_o+\alpha\lambda}\right) = 0$$

only possible for $\frac{a_o}{a_o+\alpha\lambda} = 1$ or $\alpha\lambda = 0$

This condition is not applicable.

conclusion:

The only condition which will yield $\det[A] = 0$ is $\omega = 0$

APPENDIX V

ANALYSIS OF PROTONOTARIOS AND WING[30]

A5-1 Transmission Parameters (ABCD)

$$A = 1 + \sum_{n=1}^{\infty} a_n s^n$$

$$B = \int_0^{\lambda} r(x)\,dx + \sum_{n=1}^{\infty} b_n s^n$$

$$C = s \int_0^{\lambda} c(x)\,dx + s \sum_{n=1}^{\infty} c_n s^n$$

$$D = 1 + \sum_{n=1}^{\infty} d_n s^n$$

where:

$$a_n = \int_0^{\lambda} c(x_{2n}) \int_0^{x_{2n}} r(x_{2n-1}) \cdots\cdots\cdots \int_0^{x_3} c(x_2) \int_0^{x_2} r(x_1)\,dx_1 \cdots dx_{2n}$$

$$b_n = \int_0^{\lambda} r(x_{2n+1}) \int_0^{x_{2n+1}} c(x_{2n}) \cdots\cdots \int_0^{x_3} c(x_2) \int_0^{x_2} r(x_1)\,dx_1 \cdots dx_{2n+1}$$

$$c_n = \int_0^{\lambda} c(x_{2n+1}) \int_0^{x_{2n+1}} r(x_{2n}) \cdots\cdots \int_0^{x_3} r(x_2) \int_0^{x_2} c(x_1)\,dx_1 \cdots dx_{2n+1}$$

$$d_n = \int_0^{\lambda} r(x_{2n}) \int_0^{x_{2n}} c(x_{2n-1}) \cdots\cdots\cdots \int_0^{x_3} r(x_2) \int_0^{x_2} c(x_1)\,dx_1 \cdots dx_{2n}$$

$n = 1, 2, 3, \cdots\cdots\cdots\cdots$

$r(x)$ = resistance per unit length variation function

$c(x)$ = capacitance per unit length variation function

λ = length of line

The four series are all uniformly convergent and the ABCD parameters are entire functions of s.

A5-2 The Network Function H(s)

From the definition of the transmission parameter A;

$$H(s) = \frac{1}{A(s)} = \frac{1}{1 + a_1 s + a_2 s^2 + a_3 s^3 + \cdots\cdots\cdots}$$

The network function is stable with poles in the left hand plane only. Also, the poles of the network function of an arbitrary non-uniform R-C line terminated in an R-C impedance (including open and short circuits) are all negative real.

A5-3 Time Response - Delay and Rise Time

From the theory developed by Elmore[14] the delay and rise time of the step response can be determined from the coefficients of s in the network function H(s). For a tapered R-C line:

$$T_D = a_1$$

$$T_R = \{2\pi(a_1^2 - 2a_2)\}^{\frac{1}{2}}$$

APPENDIX VI

THE OPERATIONAL AMPLIFIER[37]

The operational amplifier is a high gain d-c amplifier characterized by:

- near infinite gain
- near infinite input impedance
- near zero output impedance
- wide frequency bandwidth

Consider the following general voltage operational amplifier:

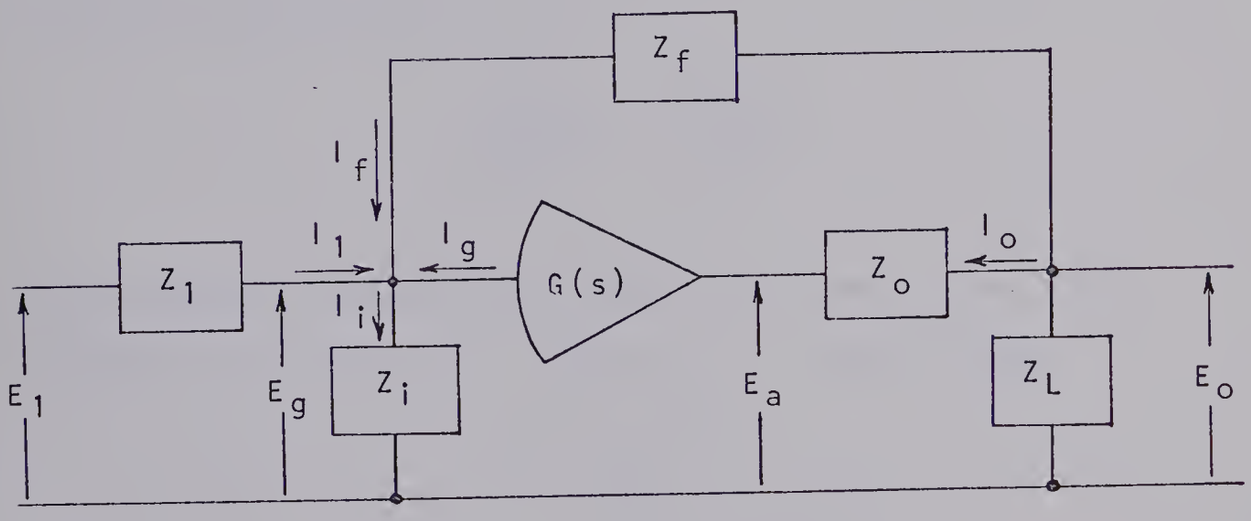

where: Z_1 and Z_f are short-circuit transfer impedances

Z_i is the input impedance

Z_o is the output impedance

Z_L is the load impedance

$G(s) = \frac{E_a(s)}{E_g(s)}$ is the transfer function of the amplifier with no load

Circuit analysis yields the following relationship:

$$\left[\frac{1}{Z_f} - \frac{1}{G} \left(\frac{1}{Z_1} + \frac{1}{Z_f} + \frac{1}{Z_i} \right) \right] E_o - \frac{Z_o}{G} \left(\frac{1}{Z_1} + \frac{1}{Z_f} + \frac{1}{Z_i} \right) I_o = - \frac{E_1}{Z_1} - I_g$$

For the conditions: $G(s) = - k$

$$Z_o = I_g = 0$$

the relationship becomes:

$$\left[\frac{1}{Z_f} + \frac{1}{k} \left(\frac{1}{Z_1} + \frac{1}{Z_f} + \frac{1}{Z_i} \right) \right] E_o = - \frac{E_1}{Z_1}$$

With k very large and Z_1, Z_f, Z_i the same order of magnitude the relationship reduces to:

$$\frac{E_o(s)}{E_1(s)} \cong - \frac{Z_f(s)}{Z_1(s)}$$

The assumptions which must hold for good operational amplifier design are:

- $G(s) \cong - k$ and k large
- $I_g \cong 0$
- Z_o very small
- Z_i large and in the order of Z_1 and Z_f

APPENDIX VII

NUMERICAL EVALUATION OF c_o

A discussion of the capacitance distribution in section 2-3 established that c(x) was constant and:

$$c(x) = c_o = 2\pi\varepsilon/\ln(r/a)$$

Numerically, assuming that the glass used is Corning 7060 Pyrex ($\varepsilon = 43.8\times10^{-12}$ fd/m) and that the ratio r/a is 1.5, we find the capacitance c_o to be 0.68 pf/mm. This is in agreement with calculations made by Nastuk and Hodgkin.[2] The value assumed for this investigation will be 1 pf/mm or 10 pf/cm.

APPENDIX VIII

NUMERICAL EVALUATION OF ρ (3MKCl)

Of specific interest here is the resistivity of the electrolyte (3MKCl) which forms the conductive path within the microelectrode. The following information was extracted from the International Critical Tables (Volume VI, page 229):

electrolyte: *3MKCl (223.68 grams dissolved in 1 litre of water)*

concentration: *C=3000 milli-moles/litre*

temperature: *18 degrees C.*

10^6 *K/C = 88.1*

K = specific conductance (ohm^{-1}-cm^{-1})

From the above information:

$$K = \frac{88.1 \times 3000}{10^6} = 0.264 \text{ ohm}^{-1}\text{-cm}^{-1}$$

Therefore: $$\rho = \frac{1}{K} = 3.78 \text{ ohm-cm @ 18 C.}$$

In this investigation the resistivity is assumed to be 4 ohm-cm.

APPENDIX IX

APPLICATION OF ROUTH'S STABILITY CRITERION[38]

The application of a Routhian array based on the characteristic equation of the closed loop transfer function of a feedback system yields information regarding system stability.

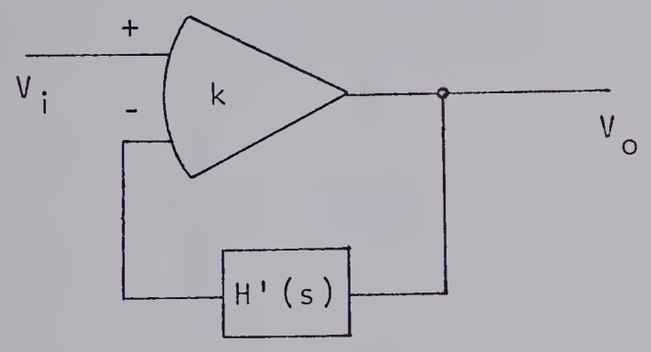

$$\frac{V_o}{V_i} = \frac{k}{1 + kH'(s)}$$

The characteristic equation is recognized as:

$$1 + k\,H'(s) = 0$$

From {3-11}:

$$H'(s) = \frac{1}{1 + a'_1 s + a'_2 s^2 + a'_3 s^3}$$

This yields the characteristic equation:

$$a'_3 s^3 + a'_2 s^2 + a'_1 s + (k+1) = 0$$

The Routhian array becomes:

$$\begin{vmatrix} a_3' & a_1' & 0 \\ a_2' & (k+1) & 0 \\ \dfrac{a_2'a_1' - a_3'(k+1)}{a_2'} & 0 & \\ (k+1) & 0 & \\ 0 & & \end{vmatrix}$$

The Routh stability criterion can be stated as follows:

"A system is stable if the Routhian array of its characteristic equation contains no negative elements in its first column."

With k a definite part of the Routhian array, the Routh criterion can be used to indicate the range of k which will give stable response.

APPENDIX X

STEP RESPONSE OF AN AMPLIFIER[39]

Under the conditions that the input to an amplifier can be represented by a single time constant low-pass network, it is possible to relate the system's rise time to the upper cutoff frequency in the following manner:

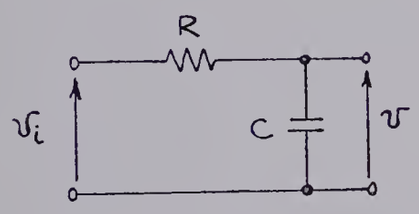

$$\tau = RC$$

$$f_{3db} = \frac{1}{2\pi\tau}$$

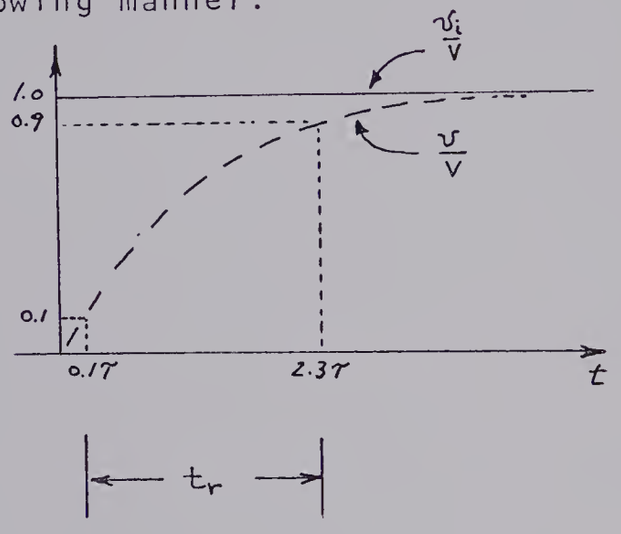

$$t_r = 2.2\,\tau = \frac{2.2}{2\pi f_{3db}} = \frac{0.35}{f_{3db}}$$

With systems which are not single time constant in nature the above relationship can be used as a first approximation of system response.